****

I give permission for public access to my thesis and for copying to be done at the discretion of the archives' librarian and/or the College library.

Gargi Mishra
Signature

05/06/2018
Date

****

Macrophage-Mediated Efferocytosis in Rat Uterine Remodeling

By

Gargi Mishra

A Paper Presented to the

Faculty of Mount Holyoke College in

Partial Fulfillment of the Requirements for

the Degree of Bachelor of Arts with

Honor

Department of Biological Sciences

South Hadley, MA 01075

May 2018

****

This paper was prepared

under the direction of

Professor Sarah J. Bacon

for eight credits.

****

****

Dedicated to all those that are brave enough to chase their dreams.

****

ACKNOWLEDGEMENTS

I would like to begin by thanking the department of Biological Sciences for supporting my research as an independent study student. I am also incredibly grateful for the support that I received from the Microscopy Society of America (MSA) for funding my immunofluorescence experiments.

I am thankful for the support that my thesis committee, comprised of Dr. Amy Camp, Dr. Kenneth Colodner, and Dr. Sarah Bacon, has provided in supporting my thesis, both at the bench and also in the writing of this paper. Special thanks to Blanca Carbajal-Gonzalez for being an invaluable resource during my fluorescence microscopy experiments and for being the person that inspired me to apply for the MSA grant funding. Thanks also to Dr. Liz Mearls, Dr. Jamie Church and Dr. Shawn Massoni for being helpful resources during some of my experiments.

I am grateful for having had the opportunity of working in professor Sarah Bacon's lab for the past three years. It has been so valuable to learn under her guidance. Going from being unsure and timid about bench research to being able to bravely design, execute, and troubleshoot experiments has been a transformation that would not have occurred if it wasn't for professor Bacon. I will miss her mentorship and hope that I can still stay in touch.

To all my friends, family, cherished advisors, professors, coaches, teammates, counselors, and mentors: a huge thank you. There are so many people in this category that I cannot even begin to describe how unconditionally supported I have felt because of you, especially when things became tough. Thank you for all that you do.

TABLE OF CONTENTS

LIST OF FIGURES

LIST OF TABLES

ABSTRACT

Macrophages are professional phagocytes that survey the body for pathogens and secrete biomolecules relevant to many cellular processes. Our lab identified the presence of macrophages around the rat uterine lumen and within the metrial gland during mid-pregnancy and postpartum. We hypothesized that macrophages might be involved in the clearance of apoptotic cells, i.e., efferocytosis. The aim of this study was to test this further. Using quantitative real-time PCR during pregnancy and postpartum timepoints, we found that the pan-macrophage marker CD68, phosphatidylserine receptor MerTK, and anti-inflammatory marker TGFβ-1 were expressed at higher levels compared to pro-inflammatory marker TNFα in the rat's metrial gland and decidua. We hypothesized that if macrophages were efferocytosing, they must be expressing MerTK. Hence, we performed double immunofluorescence across pregnancy and postpartum in the rat using frozen tissue sections containing metrial gland and decidua. Macrophages (CD68-positive) appeared spatially proximal to apoptotic cells (Annexin V-positive) and scattered in the tissue amongst perforin-positive natural killer cells. Lastly, only a few macrophages were MerTK-positive and other unknown cell types also expressed MerTK. This suggests that macrophages involved in uterine remodeling may be functionally heterogeneous. Future studies will focus on understanding how macrophages affect pregnancy in rats and whether this may have relevant implications to humans.

INTRODUCTION

Immune System Plays Important Roles During Pregnancy

A significant amount of literature testifies to the role of the immune system in facilitating a successful pregnancy. Many reports illustrate that aberrant immune function can lead to pregnancy disorders such as preeclampsia and preterm labor, which can be life-threatening to both the mother and the fetus (Perez-Sepulveda et al. 2014). Over the years, the roles of different immune cell populations in pregnancy have been actively studied.

For instance, dysregulation of Natural Killer (NK) cell and Regulatory T cell (Treg) function has been found to be predictive of early pregnancy loss (Sharma 2014). Targeting Treg cells could potentially help treat infertility (Guerin et al. 2009). A delicate balance in numbers of two distinct Dendritic cell (DC) populations has been linked to immunological tolerance during pregnancy in a mouse model system (Fang et al. 2016). The antibody-producing B cells have been shown to participate in both immune activation and suppression during pregnancy timepoints (Muzzio et al. 2013). Lastly, many monocyte subsets (Faas and de Vos 2017) and decidual macrophages have been implicated in both normal and aberrant pregnancy states (Ning et al. 2016). Our lab's primary focus is to understand the many functions that macrophages might be playing across different pregnancy timepoints.

Macrophages are well-known professional phagocytes that survey the body for pathogenic invaders and secrete biomolecules that are essential to

cellular processes involving inflammation, development, and immunogenic tolerance (Geissmann and Mass 2015). Macrophages can either be tissue-specific "resident" cells, such as brain microglia, skin Langerhans cells, or liver Kupffer cells; or be "passengers" that are monocyte-derived (originating from the bone marrow) and recruited during inflammation or during certain developmental processes in the body (Geissmann and Mass 2015). The functional hallmarks of tissue-specific subsets of resident macrophages are active areas of research by many groups that employ mouse, zebrafish, and rat genetic models of development and disease (Geissmann and Mass 2015, Garceau et al. 2015, Mathias et al. 2009).

Significance of Apoptosis and Apoptotic Cell Clearance During Pregnancy and Uterine Postpartum Involution

The embryo survives because it builds an interface with the mother that helps it obtain nutrients, get rid of metabolic wastes, and receive innate immune protection. A small subset of fetal cells called trophoblasts acquire the ability to invade the uterine wall in order for this interface to form. These fetal cells interact with maternal blood vessels called spiral arteries in order to form this interface. During this process, a lot of maternal and fetal-derived cells undergo apoptosis; their timely removal is key to ensuring that remodeling occurs fully and that the pregnancy is successful.

Spiral arteries are small arteries that during the non-pregnant luteal phase of the menstrual cycle supply blood to the endometrial lining of the uterus. They

are converted into flaccid conduits for uteroplacental blood flow during pregnancy as a result of two main physiological processes: the loss of smooth muscle cells and elastic lamina from the arterial vessel walls, and a 5-10 fold dilation of the mouths of the arteries (figure 1). These two changes are important to ensure that the mother is unable to restrict blood supply to the fetus (loss of smooth muscle cells and replacement with fibrin connective tissue) and that the blood flow does not damage the fetus (dilation of the vessels). In pathological states such as preeclampsia and fetal growth restriction, the remodeling of spiral arteries appears to be incomplete leading to fetal damage such as ischemia-reperfusion injuries that generate oxidative stress in the fetus (Burton et al. 2009).

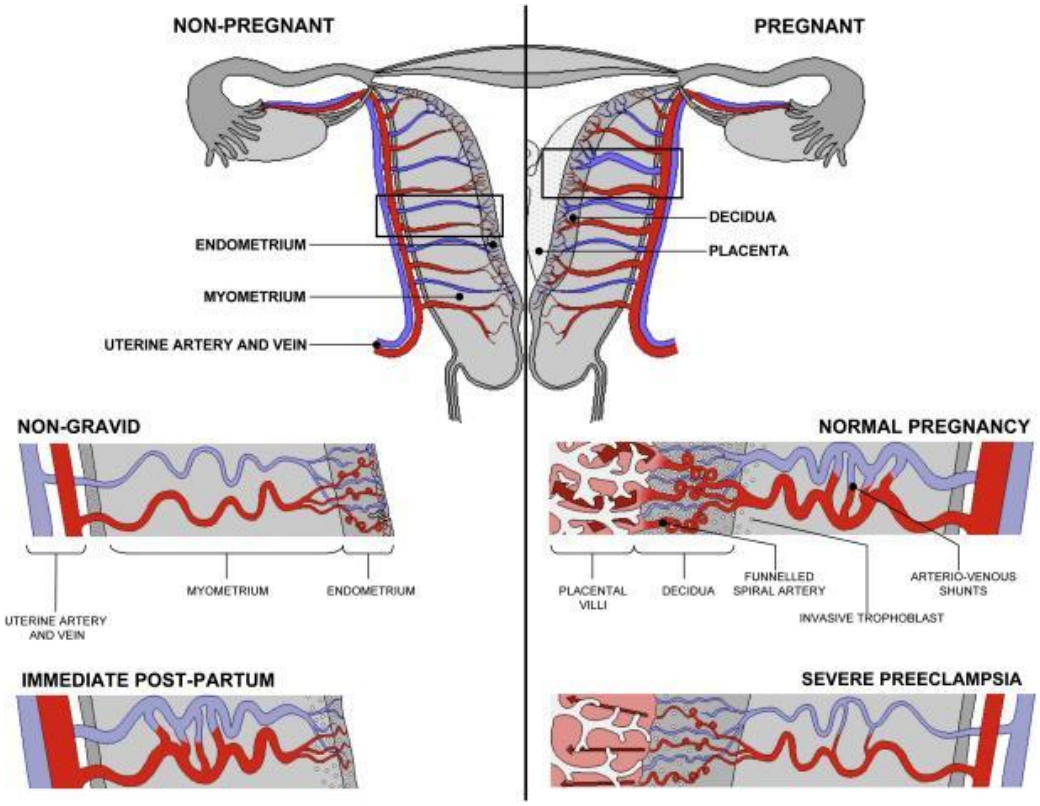

Figure 1. Different physiological states of the human uterus. Each physiological state requires remodeling of the vasculature, in which different immune cells are implicated. In the nonpregnant (non gravid) state, spiral arteries supply blood to the endometrial lining of the uterus, which is shed every month due to menstrual bleeding. In the pregnant state, the same spiral arteries become remodeled such that they lose their smooth muscle wall and elastin. They also become much more dilated, arterio-venous shunts can be seen, and the fetal trophoblast cells can be seen to have successfully invaded into the myometrial wall of the mother. At the beginning of postpartum, spiral arteries begin to be remodeled back to their non gravid state, and this phenomenon is marked by high rates of endometrial apoptosis and myometrial autophagy, in order for new spiral arteries to develop that contain elastin and a smooth muscle wall. However, during severe preeclampsia, it is clear that the remodeling is incomplete since the arteries appear narrow, the trophoblast invasion is not as deep, and fewer arterio-venous shunts have formed. Figure adapted from Burton et al. 2009.

Spiral artery remodeling occurs in two waves. In the first wave, natural killer (NK) cells associate with the spiral arteries and begin to secrete cytokines that signal the apoptosis of endothelial and vascular smooth muscle cells. These

apoptotic cells need to be engulfed before they necrotize, in order to prevent inflammation. In the second wave of arterial remodeling, extra-embryonic cells called endovascular trophoblasts invade the uterine lining traveling from the endometrial side towards the myometrium (the maternal uterine wall) and help smooth muscle cells (that have undergone cell death) be replaced by fibrin. NK cells help modulate the rate of trophoblast invasion towards the myometrial region of spiral arteries (Soares et al. 2012) (figure 2).

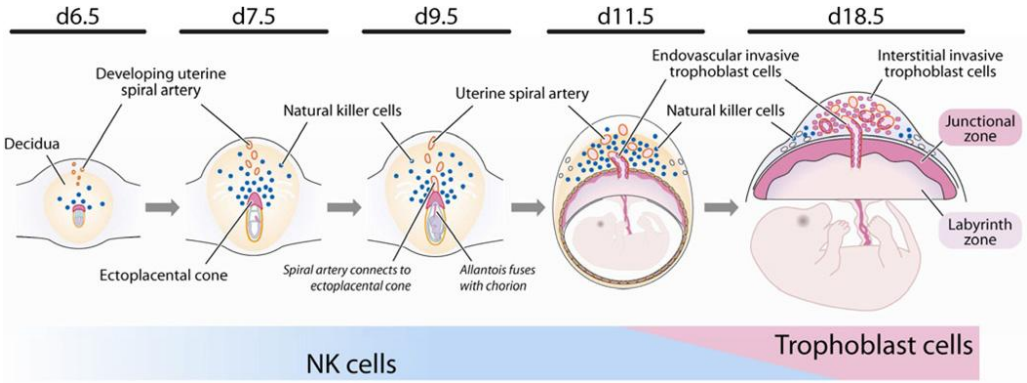

Figure 2: The role of natural killer (NK) cells in spiral artery remodeling has already been established in the literature. For instance, NK cells initiate the first wave of remodeling by secreting angiogenic factors such as VEGF, interferon-gamma (IFN-g), and nitric oxide among others that facilitate the disruption of spiral arteries (via induction of endothelial and vascular smooth muscle cell apoptosis). During the trophoblast-mediated second wave of remodeling, NK cells regulate the rate at which trophoblast cells migrate toward the maternal uterine wall. Figure adapted from Soares et al. 2012.

As these trophoblast cells migrate, some of them die via apoptotic mechanisms. Since trophoblast cells are semi-allogeneic to the mother (i.e., they express fetal antigens), if they lyse into apoptotic blebs, fetal antigens can be exposed to the mother's immune system and recognised as 'non-self' thereby leading to an inflammatory immune response which can halt further arterial

remodeling, and may even affect the growing fetus. This is why the timely and efficient phagocytosis of apoptotic maternal endothelial and vascular smooth muscle cells as well as apoptotic fetal trophoblast cells is essential for a successful pregnancy.

During uterine postpartum involution, the highly remodeled arteries and the uterine wall need to be remodeled back into a nonpregnant state. It has been shown that across many species, the rates of apoptosis in endometrial cells (modified into decidua basalis) and autophagy in myometrial cells (modified into the mesometrial triangle in the case of rodents) increase drastically during postpartum involution (Soares et al, 2012, Hsu et al. 2014). This again warrants a role for professional phagocytes such as macrophages in engulfing apoptotic cells in a timely manner to ensure that postpartum involution can progress without accumulation of necrotic tissue and a pro-inflammatory immune response.

Human and Rodent Placental Bed Abounds in Natural Killer Cells and Macrophages

Both humans and rodents possess hemochorial placentation which is the most invasive form of placentation that takes a long time to develop (Faas and de Vos 2017). In humans, the placenta takes 12-13 weeks of the 280-day (40-week) long gestation period to develop, in order to be fully able to supply blood to the fetus and remove metabolic wastes among other important functions. In mice, the placenta continues to develop till 18th day of the 21 day long gestational period. Similarly, in rats, the placenta also continues to develop throughout most of the

gestational period of 23 days. Different types of immune cells can be found in the placental bed throughout pregnancy. Due to the presence of fetal antigens (recognized as ‘non-self’ by the mother’s immune system), it is imperative that the mother’s immune responses be significantly redirected to ensure a successful pregnancy.

Moreover, successful implantation and placentation both require coordinated support from different immune cells. Leukocytes present in the decidua basalis or decidua (modified endometrium that represent the maternal part of the placenta) consist of a high population of uterine NK (uNK) cells and macrophages during the first and second trimester. The number of uNKs and macrophages decreases during the third trimester. T lymphocytes (and yet a smaller proportion of dendritic cells, B cells, and monocytes) are also present in smaller numbers throughout all stages of pregnancy (figure 3).

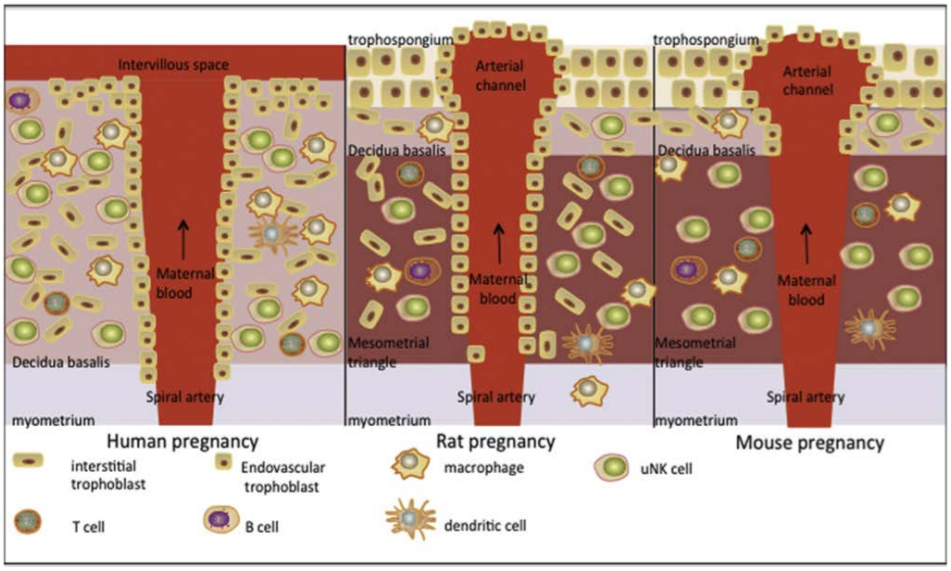

Figure 3: An overview of the fetal-maternal interface in humans, rats, and mice adapted from Faas and de Vos, 2017. It is evident that the placental beds of humans and rodents are densely populated by immune cells, the two most prominent cell types being natural killer cells and macrophages. While human placental bed only consists of the decidua basalis and the myometrium, the rodent placental beds consist of decidua basalis, mesometrial triangle and the myometrium. The mesometrial triangle contains small lymphoid aggregates called metrial glands, which comprise the mesometrial vasculature. The extent of trophoblast invasion in each of the three species is also apparent. In humans, trophoblasts invade through the decidua basalis and up till the myometrium.In mice, trophoblast invasion only proceeds till the end of the decidua basalis. But in rats, the trophoblasts invade through the decidua basalis and mesometrial triangle region to reach the beginning portion of the myometrium. This makes the rat a good model to study how spiral artery remodeling might occur in humans.

In humans, uNK cells have been shown to play roles in spiral artery remodeling via production of cytokines, growth factors and angiogenic factors. Macrophages have been shown to play a role in facilitating trophoblast invasion, and blastocyst implantation (Faas and de Vos, 2017). Their numbers increase drastically during pregnancy, with the highest density corresponding to the first two trimesters. Macrophages are in close proximity to spiral arteries with disrupted vascular smooth muscle cells and in areas where endothelial cells are

absent, which suggests that macrophages might be involved in remodeling the spiral arteries (Smith et al. 2009).

In mice, uNK cells appear to have a better characterized role to play, compared to in other rodents such as rats. In mice, uNK cells are found to be essential for arterial remodeling, since their depletion results in aberrant-looking decidual and myometrial structures during mid-pregnancy (Croy et al. 2012). In mice, the macrophages are present in the decidua throughout all pregnancy timepoints and their numbers increase at the end of the pregnancy. But their functional significance is still unclear.

In rats, macrophages are present in the decidua, and in the deeper portion of the placental bed in between the circular and longitudinal muscle layers of the myometrium, i.e., the mesometrial triangle. Macrophages in the mesometrial triangle can be found in regions called metrial glands that are small granular structures that are highly vascularized and appear in the mesometrial triangle on gestational day 8 (GD-8) and persist till parturition. Metrial glands consist of a highly heterogeneous population of cells, the most prominent being granulated metrial gland (GMG) cells, endometrial stromal cells, trophoblasts, endothelial cells that line blood vessels, fibroblasts, and some leukocytes (Picut et al. 2009). Spiral arteries are present in the rat metrial gland and it has been found that uNK and endovascular trophoblast cells are necessary for the remodeling of these arteries (Furukawa et al. 2011).

Moreover, macrophages have been reported to be present in the rat metrial gland during later time points in pregnancy (Peel et al. 1979). Macrophages are also present in the interstitium and around spiral arteries of rats, but their presence around spiral arteries does not correlate with the phenotype of a disrupted spiral artery as seen in humans. This is why there is a general agreement in the field that macrophages may not be facilitating spiral artery remodeling directly in rats. However, the role of macrophages in effectively clearing up apoptotic cells that result from processes such as spiral artery remodeling during pregnancy is highly plausible.

Rationale for this Study

The role of macrophages in clearing apoptotic cells during pregnancy in humans has been reviewed. The process appears to be active, rather than neutral, with macrophages expressing many anti-inflammatory molecules such as IL-10 and TGFβ, and suppressing TNFα production. Moreover during pathological states such as preeclampsia, macrophages have been found to induce apoptosis in trophoblast cells by actively producing proinflammatory molecules such as TNFα and IFNγ, which make trophoblast cells more susceptible to undergoing Fas-mediated apoptosis, thereby disrupting the normal remodelling process (Kyathanahalli et al. 2013). However, the molecules, expressed either by macrophages or another phagocyte during pregnancy in humans and rodents, and directly responsible for the engulfment of apoptotic cells, a process termed efferocytosis, have not been identified. The aim of this study was to identify

plausible molecules that macrophages might be utilizing in efferocytosis during pregnancy and postpartum.

We have focused our experiments on the time points of mid-pregnancy and early postpartum. A previous undergraduate student in the lab and I observed CD68-immunopositive macrophages around the rat uterine lumen and metrial gland tissue during postpartum in the rat using immunohistochemistry (data unpublished) and during gestation day 14 using quantitative qRT-PCR. These results inspired us to first study T-cell immunoglobulin and mucin domain containing-3 (Tim3), Mer Tyrosine Kinase (MerTK), Interleukin-10 (IL-10), and Transforming growth factor (TGFβ -1, or TGFβ). IL-10 and TGFβ are classical anti-inflammatory molecules expressed by macrophages. Tim3 and MerTK are both phosphatidylserine receptors known to be involved in binding phosphatidylserine moieties that get exposed on the extracellular surface of apoptotic cells, thereby facilitating phagocytosis. While Tim3 is expressed by many different immune cell types such as T-cells and NK cells, MerTK expression is highly associated with macrophages, although some uterine NK cells also express MerTK.

Both Tim3 and MerTK appear to be implicated in many biological contexts including pregnancy. In humans, a lowered percentage of Tim3-positive decidual NK cells was found to correlate with a higher frequency of miscarriages. This phenotype was found to be recapitulated in murine models of spontaneous abortion (Aschkenazi et al. 2002). Tim3, as stated previously, is also critical for

the functions performed by other immune cell populations such as macrophages, monocytes, dendritic cells, mast cells, and endothelial cells, in addition to NK cells. Tim3 responds to its ligand Galectin-9 (Gal-9) which is secreted by trophoblast cells in the context of pregnancy. Dysregulation of Gal-9/Tim3 signaling has been associated with autoimmunity, increased viral infection, and tumor invasion (Li et al. 2016).

Tim3's effect on macrophage function varies by context. Some studies suggest that Tim3 might act as an inhibitor of macrophage activation during the early stages of an immune response. On the other hand, overexpression of Tim3 in macrophages was found in cases of sepsis and LPS-induced macrophage activation. Moreover, blocking Tim3 expression decreases the phagocytic potential of uterine macrophages, leading to a build of apoptotic cells in the uterine region which leads to a local immune response. The functional role played by Tim3 appears to be two-way: up to a certain point Tim3 acts as a "brake" by inhibiting macrophage activation, but in cases of chronic inflammation, the "brake" is lifted, causing Tim3 to be overexpressed, helping the cells to remain quiescent due to "exhaustion" (Han et al. 2013).

The importance of MerTK in engulfment of apoptotic cells has been established in other biological contexts. For instance, MerTK is both necessary and sufficient for the engulfment of apoptotic pyrenocytes during enucleation of erythroid cells in order to form mature erythrocytes (Toda et al. 2014). In this setting, it is the central macrophages found in erythroblastic islands that express

MerTK. Resident peritoneal macrophages have also been shown to express MerTK and Tim4 (another family member of the TIM family and thus, highly related to Tim3), which facilitate the engulfment of apoptotic cells by recognizing and binding exposed phosphatidylserine. In order to facilitate phagocytosis, MerTK (and its other family members Axl and Tyro3) rely on small bridging molecules called ProteinS and Gas6 that help tether the receptor tyrosine kinase to the cell that needs to be engulfed (Toda et al. 2014, Dransfield 2015). More interestingly, there appears to be a functional relationship between MerTK and TGFβ function. In a human cell culture model of multiple sclerosis, it was found that TGFβ-treated microglia differentially expressed MerTK at high levels. This microglial phenotype was associated with greater phagocytosis of myelin present on co-cultured neurons of the central nervous system (Healy et al. 2016). Thus, expression of TGFβ -1 and MerTK in the metrial gland and decidual tissue during mid-pregnancy and postpartum might suggest a common cellular pathway through which these molecules act.

Aims of this Study

In this study, we characterize the steady-state expression of a subset of macrophage-associated genes in the metrial gland and decidual tissue during gestational days 12, 14, and 16 and postpartum day 3. It is hypothesized that the pan-macrophage marker CD68, phagocytic marker MerTK and anti-inflammatory marker TGFβ will have high expression during mid-pregnancy and postpartum, while the expression of proinflammatory markers such as TNFα will be low.

This study also utilizes immunofluorescence as a technique to determine whether macrophages are involved in engulfing apoptotic cells during mid-pregnancy and postpartum, and whether there is any cross-talk between macrophages and perforin-positive NK cells based on their location in the uterine tissue. It is hypothesized that MerTK expression will colocalize with that of CD68 in the uterine tissue, thereby implying that CD68-positive cells (macrophages) also express MerTK. It is also hypothesized that CD68-positive macrophages will be found in spatial proximity to Annexin V-positive apoptotic cells that they are involved in engulfing. The results of this study will contribute to increasing our understanding of how immune cell subsets such as macrophages facilitate the completion of a successful pregnancy in rat, and how pregnancy outcomes might get perturbed due to aberrant immune cell function.

METHODS

Animal Handling and Sample Collection

Prior to data collection, female Norway rats (*Rattus norvegicus*) called dams were assessed daily for three to four weeks by vaginal lavage to ascertain the part of the estrous cycle that they were in. When a dam was found to be in the estrus (ovulatory) phase, she was placed in a caged mating environment in the presence of a male Norwegian rat (sire) overnight. The next day, the dam was removed from the presence of the sire, and checked if she was sperm-positive via vaginal lavage.

The dam was sacrificed either during pregnancy (on gestation day 12, 14, or 16) or postpartum (on postpartum day 1 or 3) by CO_2-mediated asphyxiation, and dissected immediately to obtain the organs or tissues of interest. The tissues included decidua basalis, metrial gland (MG) and placenta for the mid-gestation time points and uterine wall for the virgin control and the postpartum timepoints. Tissues to be used for RNA expression analysis were homogenized in TRIZol (1 mg tissue per 1 mL TRIZol solution) and stored at -80 °C until the RNA extraction step (table 1). Tissues to be used for immunofluorescence studies were embedded in OCT, frozen immediately in liquid nitrogen and stored at -80 °C until cryosectioning (table 3).

mRNA Expression Analysis Using Quantitative Real-Time PCR

Table 1: Sample size for qRT-PCR experiments.

Time Point	**Dam IDs**
Virgin in Estrus	AD16, AD33, AD48
Gestation Day 12 (GD12)	AA03, AB03, AB04
Gestation Day 14 (GD14)	AA04, AB05, AB11
Gestation Day 16 (GD16)	AD03, AD15, AD21
Postpartum day 3 (PPD3)	AB07, AD18, AD27

RNA Extraction and Dnase-treatment:

Tissues were homogenized in TRIZol and stored at -80 °C. Prior to RNA extraction, stored tissue was thawed on ice for 5 minutes and then at room temperature for 2 minutes. RNA was extracted using chloroform, precipitated using isopropanol, pellets washed with ethanol, and the pellets resuspended in Nuclease-Free water. The crude RNA samples from the tissues were Dnase-treated using the Ambion Dnase-Free Kit.

cDNA Synthesis and Validation of cDNA Purity and Integrity:

The resulting DNase-treated RNA was used to synthesize cDNA using the enzyme reverse transcriptase (Superscript III). Control samples lacking reverse transcriptase treatment were also synthesised (noRT) to probe for genomic contamination later on. Equal amounts of Dnase-treated RNA, 4.2 ug/uL for the

earlier primer efficiency plates, and 3.7 ug/uL for experimental plates, were used in order to ensure template equality across all conditions. The reason for choosing these amounts was a result of the amount of RNA that was able to be extracted from the samples at the time of RNA extraction and Dnase-treatment. In the case of preparing samples for primer efficiency, the sample with the lowest RNA amount had a concentration of 4.2 ug/uL, while for experimental samples, the limiting sample had a concentration of 3.7 ug/uL.

The cDNA and noRT samples were used as templates in a PCR and products analysed on a gel to validate that the cDNA was free of genomic contamination and that the RNA integrity was maintained. For the samples that had huge primer dimer clouds in the cDNA lanes (suggesting loss of RNA integrity) or any presence of amplified product in noRT lanes (suggesting genomic contamination) were repeated going back to the Dnase-treatment step. The validated cDNA transcripts were then used to carry out quantitative RT-PCR (qRT-PCR).

Primer Design and Primer Efficiency Measurements Via Quantitative Real-Time PCR:

Primer sets for the genes mentioned in table 2 were tested for efficiency using cDNA samples taken from GD14 metrial gland (GD14 MG). This tissue was chosen due to availability and since GD14 was a chronologically median time point amongst all samples.

Primer sets were designed for the genes *MerTK*, *TIM3*, *IL10*, and *MRC1*, while primer sets already present in the lab were used for the genes *TGFβ1*, *TNFα*, *CD68*, and *RPL13a* (housekeeping gene). While designing primer sets, the following identical parameters were used: the primer must span an exon-exon boundary, be between 15-25 base pairs long, be intended for a PCR product size ranging from 150-250 base pairs, have an optimal melting temperature of 60 °C, and have a maximum melting temperature difference of 3.

Table 2. List of primer set sequences used.

Gene	**Gene Primer Set**	**Forward Primer**	**Reverse Primer**	**Efficiency**	**Non specific Peak Present**
TGFβ1	TGFβ1-3	5'-TGGCCAGATCCTGTCCAAAC-3'	5'-CATAGATTGCGTTGTTGCGGT-3'	111	Very minor
TNFα	TNFα -3	5'-GTAGCCCACGTCGTAGCAAA-3'	5'-AAATGGCAAATCGGCTGACG-3'	90	No
MerTK	MerTK-10	5'-GGAATTGCATGTTGCGGGAT-3'	5'-CCACATGGTCACGCCAAAAG-3'	102	No
CD68	CD68-4	5'-CCTGACCCAGGGTGGAAAAA-3'	5'-GAATGTCCACTGTGCTGCTTG-3'	102	No
RPL13a	RPL13a-2	5'-TGGTGGTTGTACGCTGTGAG-3'	5'-CTCTTTTGGTCTTGTGCGGC-3'	106	Yes
TIM3	TIM3-9	5'-CTCCCAGAACCCTAACCACTG-3'	5'-AAGAATAAGTGCCAGGGCCAG-3'	105	No
IL10	IL10-17	5'-GGTAGAAGTGATGCCCCAGG-3'	5'-TGGCCTTGTAGACACCTTTGT-3'	103	No
MRC1	MRC1-6	5'-TCAACTCTTGGACTCACGGC-3'	5'-CATGATCTGCGACTCCGACA-3'	95	Yes
SRP14	SRP14-5	5'-CCGGTTGAACCTCAGAAGGC-3'	5'-GACACTTGTTTTCTGCGGGC-3'	85	No

In order to set up primer efficiency qRT-PCR plates, GD14 MG cDNA was diluted to a 1:5 concentration and this acted as the most concentrated template. Four more dilutions were made by diluting the previous dilution by 1:10 in order to make a five-point ten-fold dilution series (figure 4). Each primer set was used on an identical but separate dilution series, standard curves were plotted and efficiencies calculated from the slope. Only those primer sets were chosen that had efficiency values between 90 and 115, and lacked a huge shoulder peak. When choosing between different primer sets for a given gene, the set that lacked a visible shoulder peak but had a slightly high efficiency value was chosen, unless the efficiency value was much greater than 115, in which case the primer set with a small shoulder peak was tolerated (this turned out to be the case for the primer set chosen for the housekeeping gene RPL13a).

Primer Set for Gene 1 Dilution 1 200 ng	Primer Set for Gene 1 Dilution 2 20ng	Primer Set for Gene 1 Dilution 3 2ng	Primer Set for Gene 1 Dilution 4 .2ng	Primer Set for Gene 1 Dilution 5 .02ng	No RT	Primer Set for Gene 2 Dilution 1 200 ng	Primer Set for Gene 2 Dilution 2 20ng	Primer Set for Gene 2 Dilution 3 2ng	Primer Set for Gene 2 Dilution 4 .2ng	Primer Set for Gene 2 Dilution 5 .02ng	No RT
Primer Set for Gene 1 Dilution 1 200 ng	Primer Set for Gene 1 Dilution 2 20ng	Primer Set for Gene 1 Dilution 3 2ng	Primer Set for Gene 1 Dilution 4 .2ng	Primer Set for Gene 1 Dilution 5 .02ng	No RT	Primer Set for Gene 2 Dilution 1 200 ng	Primer Set for Gene 2 Dilution 2 20ng	Primer Set for Gene 2 Dilution 3 2ng	Primer Set for Gene 2 Dilution 4 .2ng	Primer Set for Gene 2 Dilution 5 .02ng	No RT
Primer Set for Gene 1 Dilution 1 200 ng	Primer Set for Gene 1 Dilution 2 20ng	Primer Set for Gene 1 Dilution 3 2ng	Primer Set for Gene 1 Dilution 4 .2ng	Primer Set for Gene 1 Dilution 5 .02ng	No RT	Primer Set for Gene 2 Dilution 1 200 ng	Primer Set for Gene 2 Dilution 2 20ng	Primer Set for Gene 2 Dilution 3 2ng	Primer Set for Gene 2 Dilution 4 .2ng	Primer Set for Gene 2 Dilution 5 .02ng	No RT
Primer Set for Gene 3 Dilution 1 200 ng	Primer Set for Gene 3 Dilution 2 20ng	Primer Set for Gene 3 Dilution 3 2ng	Primer Set for Gene 3 Dilution 4 .2ng	Primer Set for Gene 3 Dilution 5 .02ng	No RT	Primer Set for Gene 4 Dilution 1 200 ng	Primer Set for Gene 4 Dilution 2 20ng	Primer Set for Gene 4 Dilution 3 2ng	Primer Set for Gene 4 Dilution 4 .2ng	Primer Set for Gene 4 Dilution 5 .02ng	No RT
Primer Set for Gene 3 Dilution 1 200 ng	Primer Set for Gene 3 Dilution 2 20ng	Primer Set for Gene 3 Dilution 3 2ng	Primer Set for Gene 3 Dilution 4 .2ng	Primer Set for Gene 3 Dilution 5 .02ng	No RT	Primer Set for Gene 4 Dilution 1 200 ng	Primer Set for Gene 4 Dilution 2 20ng	Primer Set for Gene 4 Dilution 3 2ng	Primer Set for Gene 4 Dilution 4 .2ng	Primer Set for Gene 4 Dilution 5 .02ng	No RT
Primer Set for Gene 3 Dilution 1 200 ng	Primer Set for Gene 3 Dilution 2 20ng	Primer Set for Gene 3 Dilution 3 2ng	Primer Set for Gene 3 Dilution 4 .2ng	Primer Set for Gene 3 Dilution 5 .02ng	No RT	Primer Set for Gene 4 Dilution 1 200 ng	Primer Set for Gene 4 Dilution 2 20ng	Primer Set for Gene 4 Dilution 3 2ng	Primer Set for Gene 4 Dilution 4 .2ng	Primer Set for Gene 4 Dilution 5 .02ng	No RT

Figure 4: Plate design used for determining the efficiency of primer sets used for subsequent experiments.

mRNA Expression Analysis for the genes *CD68*, *TNFα*, *TGFβ*, and *MerTK*:

RPL13a acted as the housekeeping (normalising) gene, while virgin uterus was used as control tissue. Each sample (cDNA and noRT) was diluted to a 1:4 concentration (since the starting Dnase-treated RNA amount prior to cDNA synthesis had been 3.7 ug/uL as opposed to more than 4 ug/uL). Each template was used in triplicates for the four experimental primer sets (CD68, TNFα, TGFβ, and MerTK). In addition to being the housekeeping gene, RPL13a also acted as the gene that was used to detect any low levels of genomic contamination present in the noRT samples (figure 5). No template controls (NTC) using water were

also run in order to identify any primer dimer clouds or contamination in the primer sets.

GD12 MG CD68	GD12 MG CD68	GD12 MG CD68	GD12 MG MerTK	GD12 MG MerTK	GD12 MG MerTK	GD12 MG RPL13a-2	GD12 MG RPL13a-2	GD12 MG RPL13a-2	GD12 MG RPL13a-2 no RT	GD12 MG RPL13a-2 no RT	GD12 MG RPL13a-2 no RT
GD14 MG CD68	GD14 MG CD68	GD14 MG CD68	GD14 MG MerTK	GD14 MG MerTK	GD14 MG MerTK	GD14 MG RPL13a-2	GD14 MG RPL13a-2	GD14 MG RPL13a-2	GD14 MG RPL13a-2 no RT	GD14 MG RPL13a-2 no RT	GD14 MG RPL13a-2 no RT
GD16 MG CD68	GD16 MG CD68	GD16 MG CD68	GD16 MG MerTK	GD16 MG MerTK	GD16 MG MerTK	GD16 MG RPL13a-2	GD16 MG RPL13a-2	GD16 MG RPL13a-2	GD16 MG RPL13a-2 no RT	GD16 MG RPL13a-2 no RT	GD16 MG RPL13a-2 no RT
PPD3 Uterus CD68	PPD3 Uterus CD68	PPD3 Uterus CD68	PPD3 Uterus MerTK	PPD3 Uterus MerTK	PPD3 Uterus MerTK	PPD3 Uterus RPL13a-2	PPD3 Uterus RPL13a-2	PPD3 Uterus RPL13a-2	PPD3 Uterus RPL13a-2 no RT	PPD3 Uterus RPL13a-2 no RT	PPD3 Uterus RPL13a-2 no RT
GD12 Decidua CD68	GD12 Decidua CD68	GD12 Decidua CD68	GD12 Decidua MerTK	GD12 Decidua MerTK	GD12 Decidua MerTK	GD12 Decidua RPL13a-2	GD12 Decidua RPL13a-2	GD12 Decidua RPL13a-2	GD12 Decidua RPL13a-2 no RT	GD12 Decidua RPL13a-2 no RT	GD12 Decidua RPL13a-2 no RT
GD14 Decidua CD68	GD14 Decidua CD68	GD14 Decidua CD68	GD14 Decidua MerTK	GD14 Decidua MerTK	GD14 Decidua MerTK	GD14 Decidua RPL13a-2	GD14 Decidua RPL13a-2	GD14 Decidua RPL13a-2	GD14 Decidua RPL13a-2 no RT	GD14 Decidua RPL13a-2 no RT	GD14 Decidua RPL13a-2 no RT
GD16 Placenta CD68	GD16 Placenta CD68	GD16 Placenta CD68	GD16 Placenta MerTK	GD16 Placenta MerTK	GD16 Placenta MerTK	GD16 Placenta RPL13a-2	GD16 Placenta RPL13a-2	GD16 Placenta RPL13a-2	GD16 Placenta RPL13a-2 no RT	GD16 Placenta RPL13a-2 no RT	GD16 Placenta RPL13a-2 no RT
Mixed Virgin Uterus CD68	Mixed Virgin Uterus CD68	Mixed Virgin Uterus CD68	Mixed Virgin Uterus MerTK	Mixed Virgin Uterus MerTK	Mixed Virgin Uterus MerTK	Mixed Virgin Uterus RPL13a-2	Mixed Virgin Uterus RPL13a-2	Mixed Virgin Uterus RPL13a-2	Mixed Virgin Uterus RPL13a-2 no RT	Mixed Virgin Uterus RPL13a-2 no RT	Mixed Virgin Uterus RPL13a-2 no RT

Figure 5: Plate design used for determining the expression fold change of different genes normalized to the control gene RPL13a.

Immunofluorescence Analysis

Table 3: Sample size for immunofluorescence experiments.

Time Point	**Dam ID**
Virgin in Estrus	AD05
Gestation Day 12 (GD12)	AB03
Gestation Day 16 (GD16)	AD03
Postpartum day 3 (PPD3)	AB07

<u>Cryosectioning of OCT-Embedded Tissues:</u>

Tissues embedded in OCT and stored at -80 °C were allowed to equilibrate to -20 °C overnight. The tissue blocks were then sectioned using the cryostat at an optimal temperature ranging between -14 °C and -20 °C (depending

on tissue-type and time point). 6 um-thick sections were obtained on Superfrost Plus slides.

Pre-staining slide preparation:

The slides containing the tissue sections were equilibrated to room temperature (RT) for 15-30 minutes and then treated with freshly-made 2% paraformaldehyde (PFA, EM grade) made in 1X phosphate buffered saline (PBS) for ten minutes. The fixed slides were then washed thrice for 5-7 minutes each to remove excess fixative.

Antibody Optimizations:

Optimizations were mostly performed on rat spleen sections (for CD68) and some on PPD3 uterus (for MerTK). An Alexa Fluor 488 nm (AF488) conjugated primary antibody raised in mouse against rat (Bio-Rad) was used to stain for the pan-macrophage marker CD68. The isotype control was a mouse IgG conjugated to AF488. A range of antibody dilutions (1:20, 1:100, 1:200, and 1:400) were tested. A dilution between 1:20 and 1:100 gave a good signal-to-noise ratio for the CD68 protein. Hence, most subsequent CD68 stainings were carried out at a 1:50 dilution of the primary antibody. An unconjugated primary antibody raised in rabbit against rat (Fabgennix) was used to stain for the phagocytic marker MerTK. The primary antibody control used was a rabbit IgG. The secondary antibody (goat anti-rabbit) was conjugated to Alexa Fluor 594 nm (Goat Anti-Rabbit-AF594).

The secondary antibody dilution was kept fixed at 1:100, while the primary antibody was used at a range of dilutions (1:50, 1:100, 1:200, and 1:400). Results suggested that a 1:50 dilution of the MerTK primary antibody worked best and this dilution was used in all subsequent stainings. No additional optimizations were performed for the unconjugated primary antibodies rabbit anti-rat Perforin (Torrey Pines Biolabs) and rabbit anti-rat Annexin V (Abcam), which were both used at a concentration of 1:50, following company recommendations. Many blocking and antibody diluent conditions were also tested to troubleshoot non-specific staining and autofluorescence issues. It was determined that 5% normal goat serum diluted in (5% NGS) acted as an efficient blocking buffer, while 1X PBS containing 0.1% Saponin acted as an excellent antibody diluent.

Protocol for Single and Double Staining:

As noted above, prior to any staining, slides were fixed using freshly-made 2% PFA and washed extensively. Slides were then blocked using 5% NGS for an hour at RT. Immediately after blocking, the slides were incubated overnight at 4C in either a single primary antibody (for instance CD68) or a primary antibody "cocktail" containing mouse anti-rat CD68-AF488 and one of the three rabbit anti-rat antibodies (MerTK, Perforin, or Annexin V) in order to perform double staining (table 4). After the overnight primary incubation, the slides were washed thrice for 5 minutes each and then incubated with the goat anti-rabbit AF594 secondary antibody for an hour at RT (if staining for MerTK, Perforin, or

Annexin V). After secondary antibody incubation, the slides were washed twice, and incubated with Hoechst (1:2000 dilution prepared in 1X PBS) for 5 minutes at RT in order to stain for nuclei. The slides were then washed once and mounted using Prolong Diamond Antifade Glycergel (Thermo Fisher Scientific). The glycergel was allowed to cure for 24 hours, and the slides were hence imaged the following day using a fluorescence microscope.

Table 4. Immunofluorescence double-stainings performed in this study and the rationale behind each double-staining.

Antibody 1	**Antibody 2**	**Rationale**
CD68-AF488 Conjugated (mouse)	MerTK Unconjugated (rabbit)	To test whether macrophages express a phagocytic receptor.
CD68-AF488 Conjugated (mouse)	Annexin V Unconjugated (rabbit)	To test whether macrophages are spatially proximal to apoptotic cells.
CD68-AF488 Conjugated (mouse)	Perforin Unconjugated (rabbit)	To determine the proximity and relative location of macrophages with respect to natural killer cells.

MATERIALS USED IN THIS STUDY

Table 5. Reagents for RNA work and qRT-PCR

Reagent	**Purpose**
TRIZol, 2-Propanol, 95% Ethanol	RNA Extraction
Thermo Fisher Scientific DNA-free Kit	Dnase-treatment
Thermo Fisher Scientific SuperScript III First-Strand Synthesis System	cDNA Synthesis
BioRad iTaq Universal SYBR Green	qRT-PCR

Table 6. Reagents for Immunofluorescence Studies

Reagent	**Purpose**
EM-Grade 16% Paraformaldehyde	Fixation
Sigma Aldrich 10X Phosphate Buffered Saline	Buffer
Sigma Aldrich Saponin	Detergent (Membrane Permeabilization)
Jackson Immunoresearch Normal Goat Serum	Blocking Solution
Bio-Rad Mouse Anti-Rat CD68-AF488 (Clone: ED1)	Conjugated Antibody for CD68 detection
Bio-Rad Mouse IgG AF488	Isotype (Negative) Control for CD68
Fabgennix Rabbit Anti-Rat MerTK C-Epitope (Polyclonal)	Unconjugated Primary Antibody for MerTK detection
Abcam Rabbit Anti-Rat Annexin V	Unconjugated Primary Antibody for Annexin V detection
Torrey Pines Labs Rabbit Anti-Rat Perforin (Clone: Mouse CTL)	Unconjugated Primary Antibody for Perforin detection
Jackson Immunoresearch Goat Anti-Rabbit IgG AF594 (H+L)	Goat Secondary Antibody for Rabbit Antigen

Jackson Immunoresearch Rabbit IgG	Isotype Control for Rabbit Host
Thermo Fisher Scientific Prolong Diamond Antifade Mountant	Mounting Medium

RESULTS

Testing for Genomic Contamination and RNA Integrity Prior to qPCR

Two levels of precaution were used to prevent the erroneous amplification of genomic DNA in the qPCR reactions. First, primers were chosen that amplified across exon-exon spanning junctions, decreasing the likelihood that the primers could amplify intron-containing genomic DNA. Second, in the cDNA synthesis, we ran a set of identical synthesis reactions lacking the reverse transcriptase (RT) enzyme. These “no RT” samples should contain no DNA, and in a PCR, there should be no amplified product. The electrophoresis gels shown in figure 6 illustrate these data. Indeed, our no RT control samples showed no amplification, suggesting that the amplified product in the experimental lanes was due to the presence of cDNA, and not due to genomic contamination. Moreover, in situations where RNA had degraded prior to cDNA synthesis (cDNA lane AB4 and AA4 in figure 6b, or AD10 and AD27 in figure 6c), then RNA was again extracted from those tissue samples, Dnase-treated, cDNA synthesized and checked by PCR (figure 6d) in order to make sure there was no genomic contamination and that the RNA integrity had been maintained.

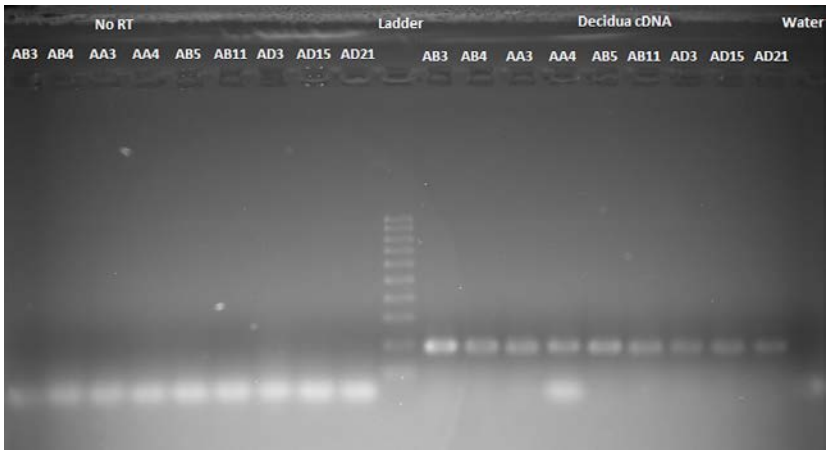
No RT
Ladder
Decidua cDNA
Water
AB3 AB4 AA3 AA4 AB5 AB11 AD3 AD15 AD21
AB3 AB4 AA3 AA4 AB5 AB11 AD3 AD15 AD21

6a

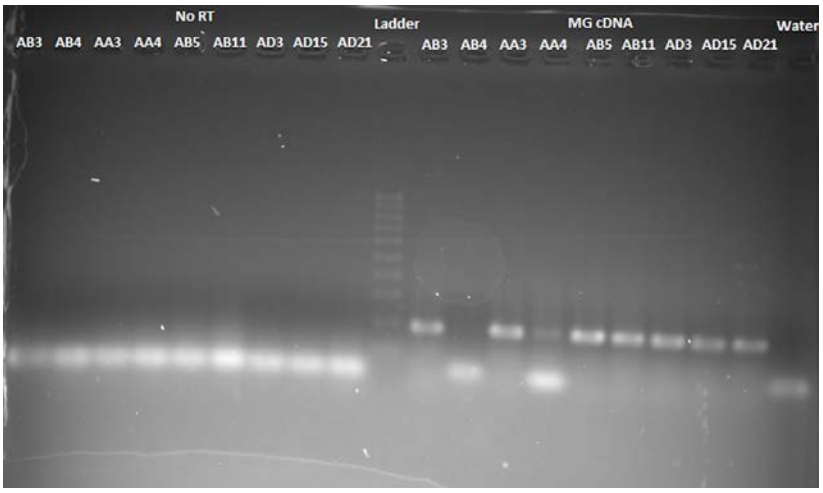
No RT
Ladder
MG cDNA
Water
AB3 AB4 AA3 AA4 AB5 AB11 AD3 AD15 AD21
AB3 AB4 AA3 AA4 AB5 AB11 AD3 AD15 AD21

6b

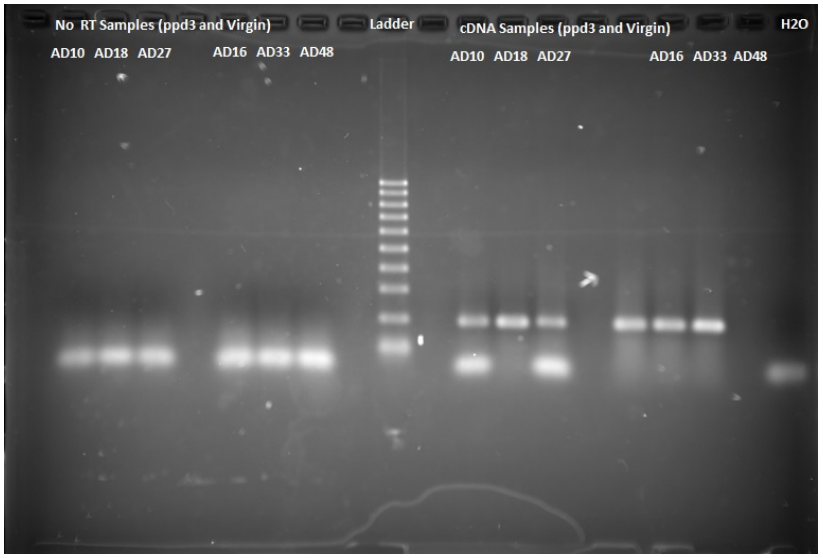
No RT Samples (ppd3 and Virgin)
Ladder
cDNA Samples (ppd3 and Virgin)
H2O
AD10 AD18 AD27 AD16 AD33 AD48
AD10 AD18 AD27 AD16 AD33 AD48

6c


No RT
AB04 AA04 AB07 AD27
Ladder
cDNA
AB04 AA04 AB07 AD27 Water

6d

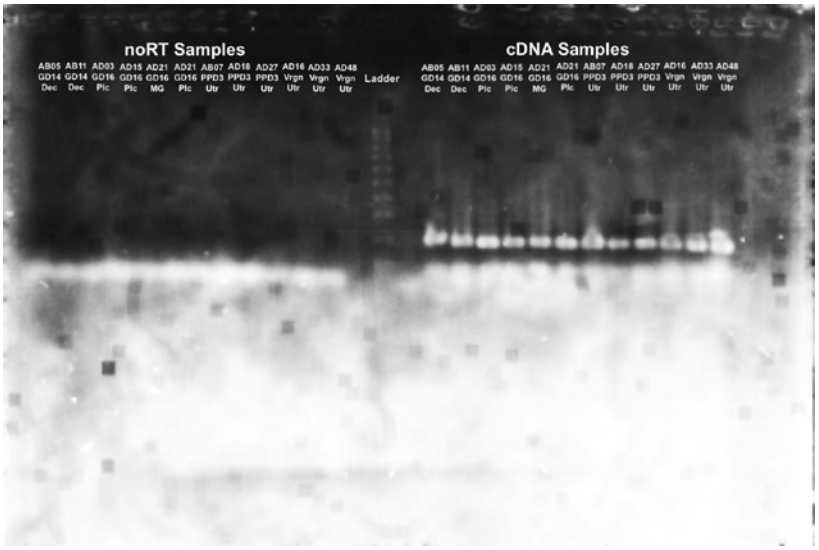
noRT Samples
AB05 GD14 Dec
AB11 GD14 Dec
AD03 GD16 Plc
AD15 GD16 Plc
AD21 GD16 MG
AD21 GD16 Plc
AB07 PPD3 Utr
AD18 PPD3 Utr
AD27 PPD3 Utr
AD16 Vrgn Utr
AD33 Vrgn Utr
AD48 Vrgn Utr
Ladder
cDNA Samples
AB05 GD14 Dec
AB11 GD14 Dec
AD03 GD16 Plc
AD15 GD16 Plc
AD21 GD16 MG
AD21 GD16 Plc
AB07 PPD3 Utr
AD18 PPD3 Utr
AD27 PPD3 Utr
AD16 Vrgn Utr
AD33 Vrgn Utr
AD48 Vrgn Utr

6e

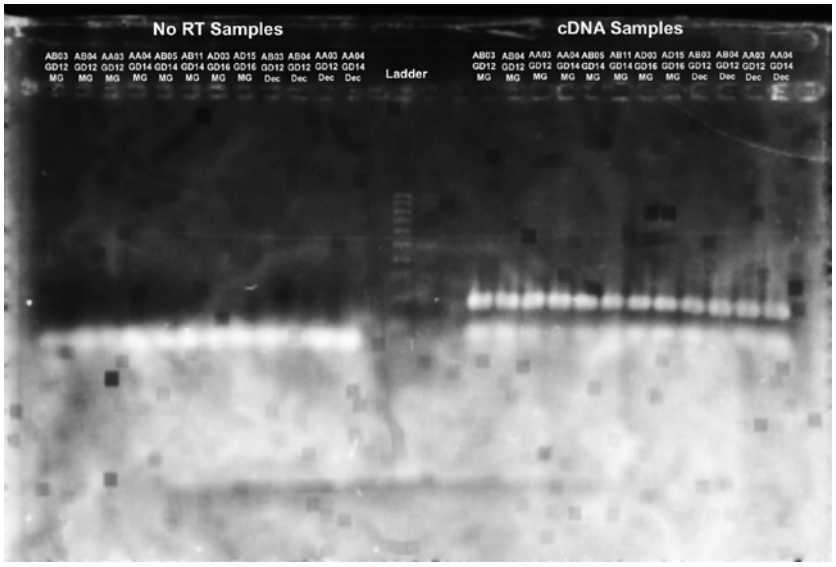

6f

Figure 6. RPL13a-2 primer PCR showing PCR products of the noRT (left) cDNA (right) synthesized from all samples for all tissues and time points used in this experiment. The samples were as follows: (a) Gestation day (GD)12, 14 and 16 Decidua, (b) GD12, 14, and 16 Metrial Gland (MG), (c) Postpartum day 3 (PPD3) and Virgin used for CD68 and MerTK qRT-PCRs; (d) repeated PCR for samples in which RNA had lost integrity or been contaminated; (e) GD12, 14, and 16 Decidua, PPD3 and Virgin Uterus, and (f) GD12, 14, and 16 MG used for TNFα and TGFβ qRT-PCRs.

Phosphatidylserine receptor Tim3 did not follow a similar expression pattern to CD68 and MerTK during pregnancy

Having confirmed that our cDNA samples lacked genomic contamination, we then set out to identify the most promising genes to analyze using qPCR. In preliminary experiments, involving only one animal per time point and not using any control tissue cDNA, we were able to only calculate a ΔCt value as opposed to a ΔΔCt value of log fold change.

Although we were only measuring ΔCt values normalized to the expression of the housekeeping gene RPL13a in the tissues of interest, these preliminary experiments still helped narrow down the genes we would analyze for

subsequent experiments. For instance, we found that CD68 (figure 7a) was expressed in the metrial gland on days 12, 14, and 16; in the decidua on day 14 during pregnancy; and also on postpartum day 3. MerTK (figure 7b) and Tim3 (figure 7c) were also expressed at each of the time point studied, but at much lower levels in relation to CD68.

Another striking observation was that in comparison to the expression levels of the genes CD68 (figure 7a) and MerTK (figure 7b) the expression of Tim3 (figure 7c) did not follow a similar pattern. For instance, both CD68 and MerTK appeared to gradually increase in expression moving from days 12 through 16 of pregnancy and being very high on postpartum day 3. Tim3 on the other hand, appeared to have the highest expression on days 12 and 14 of pregnancy and was quite low on postpartum day 3. Due to this we concluded that Tim3 expression may not be specific to macrophages, consistent with what the literature also suggests; while the correspondence between CD68 and MerTK made MerTK seem a more macrophage-specific candidate to pursue. This is why further analysis of Tim3 was halted.

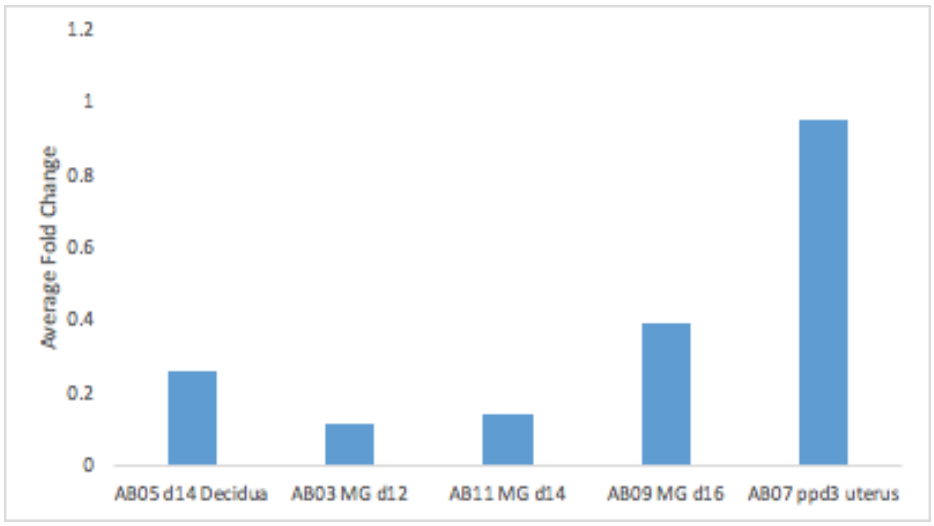

7a: CD68

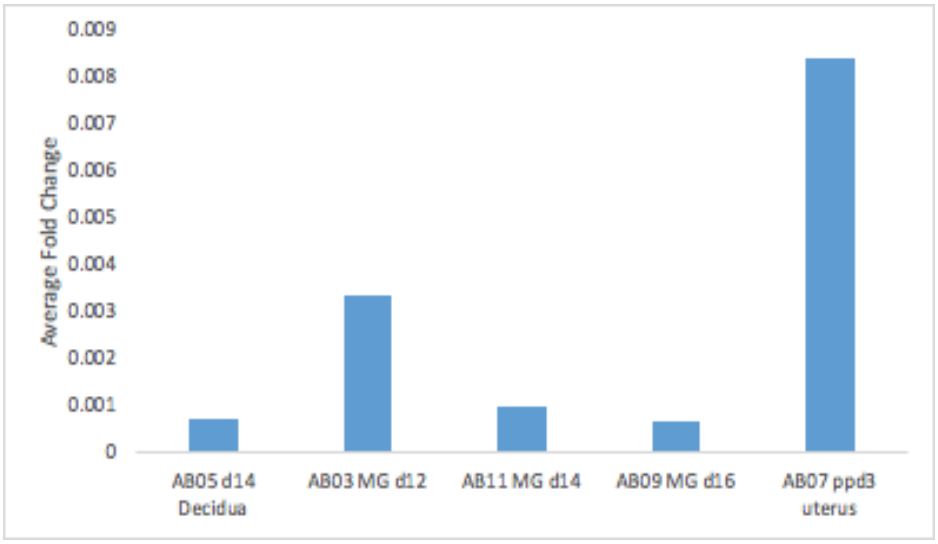

7b: MerTK

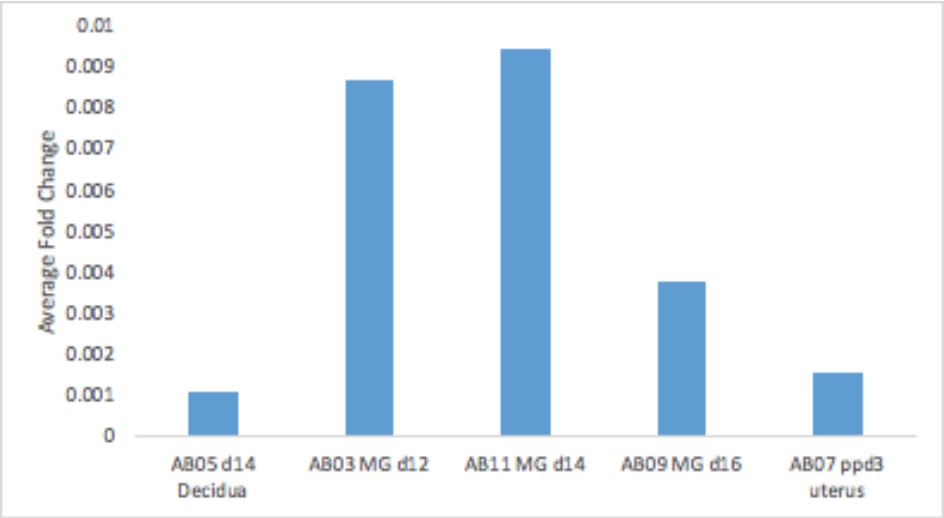

7c: Tim3

Figure 7: CD68, MerTK, and Tim3 expression normalized to RPL13a expression in the experimental tissue types and time points. Only one animal was used per condition. The average fold change represents the experimental ΔCt value calculated using RPL13a as the housekeeping gene. The ΔΔCt value could not be calculated since no control tissue (eg. virgin cDNA) was available during these preliminary experiments. CD68 and MerTK mRNA levels were both highest on postpartum day 3, while Tim3 mRNA appeared to be highest on gestation day 14 in the metrial gland.

Steady-state mRNA levels of CD68 and MerTK suggested that both CD68 and MerTK are expressed during mid-pregnancy and postpartum

The goal of our next set of qRT-PCR experiments was to quantify the mRNA expression levels of genes in uterine tissue found in pregnancy and postpartum in comparison to that in virgin uterus. Hence, after conducting preliminary experiments on samples representing only one sample per time point, we repeated the qRT-PCR experiments using three animals per tissue and time point and utilizing virgin uterus cDNA as control tissue in order to calculate ΔΔCt values, based on the plate setup described in the methods (figure 5).

Our qRT-PCR results revealed that CD68 mRNA increases gradually from

day 12 through day 16, being maximal in the uterus on postpartum day 3 (figure 8). On the other hand, MerTK mRNA appears to be low during mid-pregnancy, but is highest on postpartum day 3 (figure 9). These results are consistent with known literature that macrophages are present at different time points –validated by CD68 expression peaking in the latter half of pregnancy and in postpartum.

MerTK does not appear to be highly expressed during mid-pregnancy but its high expression during postpartum suggests that it may be facilitating the engulfment of apoptotic cells during postpartum remodeling. Hence, the high expression of both CD68 and MerTK in postpartum uterus suggests that one responsibility of macrophages during uterine remodeling may be the efferocytosis of apoptotic cells. However, the macrophages that are present during placental development (i.e., mid-pregnancy) may not have an efferocytic role to play, consistent with the low MerTK expression.

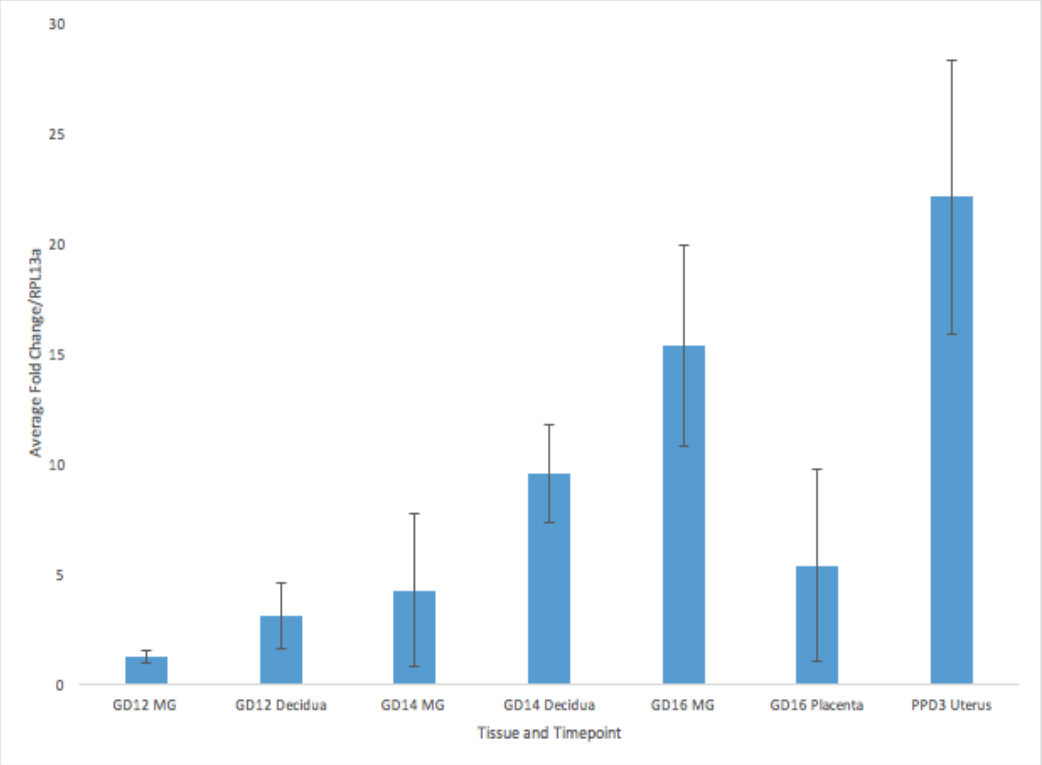

Figure 8. CD68 mRNA levels quantified via qRT-PCR. Three animals were used per condition. Error bars represent standard deviation. Virgin uterus cDNA was used as control tissue, and RPL13a acted as the housekeeping gene to which CD68 mRNA levels were normalized. CD68 mRNA levels appeared to increase as pregnancy progressed from day 12 to 16, and were very high on postpartum day 3.

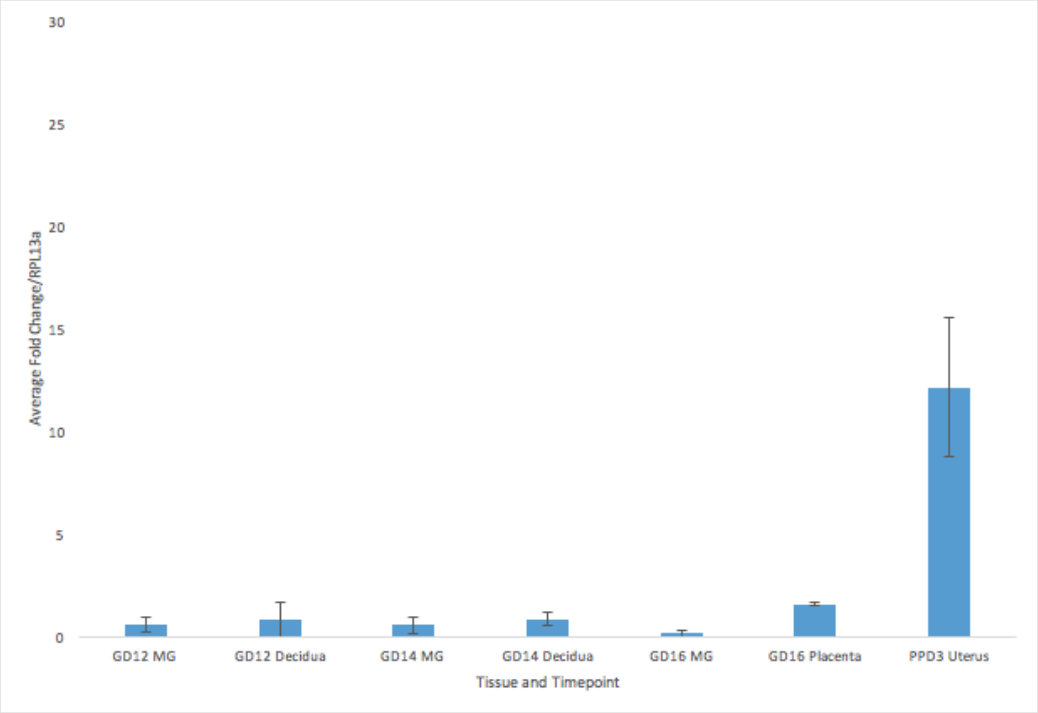

Figure 9. MerTK mRNA levels quantified via qRT-PCR. Three animals were used per condition. Error bars represent standard deviation. Virgin uterus cDNA was used as control tissue, and RPL13a acted as the housekeeping gene to which MerTK mRNA levels were normalized. MerTK mRNA was expressed at moderate levels during pregnancy but was particularly high on postpartum day 3 in the uterus. This expression pattern partially resembled that of CD68.

Steady-state mRNA levels of TNFα and TGFβ suggested that the uterine microenvironment was predominantly immunosuppressive during mid-pregnancy and postpartum

We assessed the levels of pro- and anti-inflammatory cytokines in pregnant and postpartum uterus in order to compare our findings to what is already generally understood about the microenvironment of the pregnant uterus. Consistent with the literature, the uterine tissue microenvironment was particularly immunosuppressive rather than inflammation-inducing as illustrated by the high expression of an anti-inflammatory marker TGFβ on all time points in

mid-pregnancy and postpartum (figure 10), while the levels of a pro-inflammatory marker TNFα (figure 11) were correspondingly low in pregnancy and postpartum in comparison to TGFβ.

These results from qRT-PCR studies suggest that the immunological state of the uterine region is maintained to be highly anti-inflammatory, illustrated by the high TGFβ and low TNFα levels, and this may be important for the spiral artery remodeling that occurs in the region during pregnancy. However, the slightly higher levels of TNFα on postpartum day 3, relative to the control virgin uterine tissue suggest a mechanism to prevent infections during postpartum uterine involution that occurs right after birth in the rat. But even though TNFα expression is high on postpartum day 3, TGFβ expression on postpartum day 3 is higher in comparison to it.

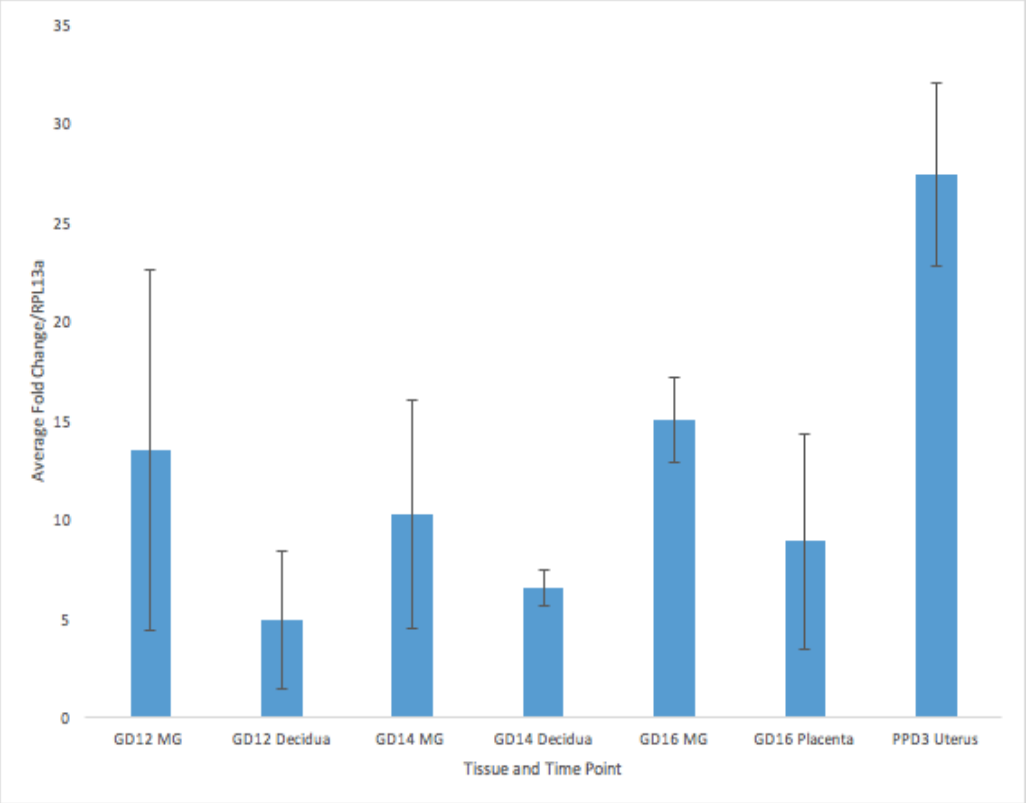

Figure 10. TGFβ mRNA levels quantified via qRT-PCR. Three animals were used per condition. Error bars represent standard deviation. Virgin uterus cDNA was used as control tissue, and RPL13a acted as the housekeeping gene to which TGFβ mRNA levels were normalized. TGFβ was expressed at high levels at all time points studied during pregnancy and postpartum.

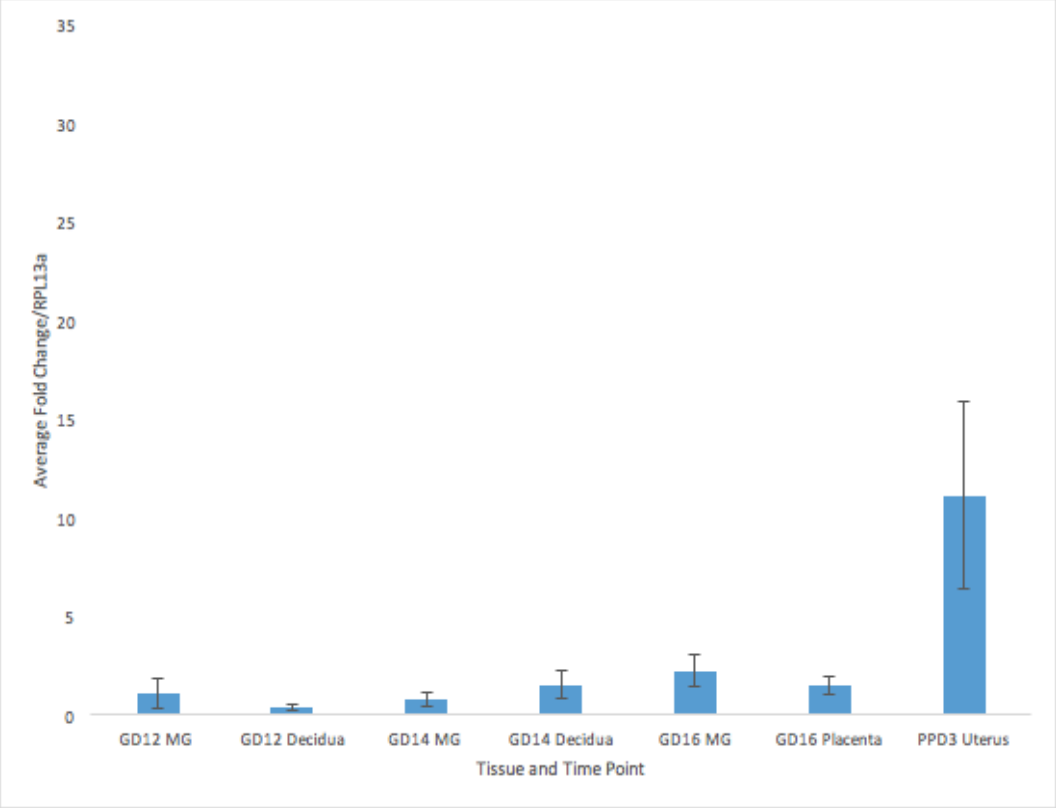

Figure 11. TNFα mRNA levels quantified via qRT-PCR. Three animals were used per condition. Error bars represent standard deviation. Virgin uterus cDNA was used as control tissue, and RPL13a acted as the housekeeping gene to which TNFα mRNA levels were normalized. TNFα levels appeared consistently low during pregnancy, but appeared to be relatively higher on postpartum day 3.

Immunofluorescence analysis suggested spatial proximity between macrophages and apoptotic cells, a small percentage of MerTK+ macrophages, and possible cross-talk between macrophages and Natural Killer cells during GD16

First, we looked for the macrophage-specific marker CD68 and the apoptosis marker Annexin V. We found that $CD68^+$ cells were near Annexin V^+ apoptotic cells (ACs) across all 5 time points, namely the Virgin (figures 12 and 19), GD12, GD16, PPD1, and PPD3 in both the decidua (figures 13, and 19-23)

and the metrial gland (figures 14 and 19-23). This suggested that macrophages might be involved in engulfing ACs via binding to phosphatidylserine moieties exposed on the surface of ACs.

Next, we looked at the potential colocalization of the phosphatidylserine receptor MerTK and the macrophage marker CD68. Were macrophages expressing MerTK? In a small percentage of cases, CD68 and MerTK colocalized to the same cell type. This was particularly significant in the Virgin endometrium (figures 12 and 19)**,** in the decidua on GD12 (figures 15 and 20) and in the decidua on PPD1 (figures 15 and 22). But, CD68 and MerTK did not colocalize during any of the time points in the metrial gland (figures 16 and 20-23), nor in the decidua on GD16 and PPD3 (figures 15, 21, and 23). MerTK was also expressed by other unknown cell types that morphologically appeared to be endothelial cells (figures 12, 15, 16, and 19-23).

Finally, knowing that both macrophage and Natural Killer (NK) cells have roles in uterine remodeling, we looked to see if the CD68 marker appeared close to a marker for NK cells, namely, the pore-forming protein perforin. Macrophages and perforin^{+} NK cells usually appeared to be present in distinct regions of virgin endometrium (figure 12) and gestational or postpartum decidual tissue (figure 17). For instance, macrophages can be seen in the lumen of blood vessels and perforin^{+} NKs are mainly seen interspersed within the decidual tissue architecture (figure 17). In the case of the mesometrial triangle region, macrophages and NK cells appeared to be scattered across the developing metrial

gland during GD12 and 16 (figures 18, 20 and 21). However, during PPD1 and PPD3, macrophages populated the periphery of the leftover metrial gland tissue while NK cells appeared to be scattered throughout (figure 18, 22, and 23).

Another interesting trend was seen in the metrial gland region on GD16, where perforin^{+} NK cells appear in high spatial proximity to CD68^{+} macrophages (figures 18 and 21). These perforin^{+} NK cells in the metrial gland on GD16 might be granulated metrial gland (GMG) cells. Hence, this proximity between CD68^{+} and perforin^{+} cells suggests a possible cross-talk between macrophages and GMG cells.

Figure legends for Immunofluorescence Images

Figure 12. Virgin endometrium at 10X magnification. First column shows the merge of immunofluorescent channels, and the second column merges the immunofluorescent channels with the phase channel. DAPI in blue (nuclear stain), FITC in green, and mCherry in red. The first row shows CD68 (FITC) and Annexin V (mCherry) double immunofluorescence; second row CD68 (FITC) and MerTK (mCherry); and the third row shows CD68 (FITC) and Perforin (mCherry). Scale bar, 100 um.

Figure 13. CD68 and Annexin V co-stains in Decidua at 10X magnification. First column shows the merge of immunofluorescent channels, and the second column merges the immunofluorescent channels with the phase channel. DAPI in blue (nuclear stain), FITC in green, and mCherry in red. All four rows represent CD68 (FITC) and Annexin V (mCherry) double immunofluorescence at different time points in the decidua (from top to bottom): GD12, GD16, PPD1, PPD3. Scale bar, 100 um.

Figure 14. CD68 and Annexin V co-stains in Metrial gland at 10X magnification. First column shows the merge of immunofluorescent channels, and the second column merges the immunofluorescent channels with the phase channel. DAPI in blue (nuclear stain), FITC in green, and mCherry in red. All four rows represent

CD68 (FITC) and Annexin V (mCherry) double immunofluorescence at different time points in the metrial gland (from top to bottom): GD12, GD16, PPD1, PPD3. Scale bar, 100 um.

Figure 15. CD68 and MerTK co-stains in Decidua at 10X magnification. First column shows the merge of immunofluorescent channels, and the second column merges the immunofluorescent channels with the phase channel. DAPI in blue (nuclear stain), FITC in green, and mCherry in red. All four rows represent CD68 (FITC) and MerTK (mCherry) double immunofluorescence at different time points in the decidua (from top to bottom): GD12, GD16, PPD1, PPD3. Scale bar, 100 um.

Figure 16. CD68 and MerTK co-stains in Metrial gland at 10X magnification. First column shows the merge of immunofluorescent channels, and the second column merges the immunofluorescent channels with the phase channel. DAPI in blue (nuclear stain), FITC in green, and mCherry in red. All four rows represent CD68 (FITC) and MerTK (mCherry) double immunofluorescence at different time points in the metrial gland (from top to bottom): GD12, GD16, PPD1, PPD3. Scale bar, 100 um.

Figure 17. CD68 and Perforin co-stains in Decidua at 10X magnification. First column shows the merge of immunofluorescent channels, and the second column merges the immunofluorescent channels with the phase channel. DAPI in blue (nuclear stain), FITC in green, and mCherry in red. All four rows represent CD68 (FITC) and Perforin (mCherry) double immunofluorescence at different time points in the decidua (from top to bottom): GD12, GD16, PPD1, PPD3. Scale bar, 100 um.

Figure 18. CD68 and Perforin co-stains in Metrial gland at 10X magnification. First column shows the merge of immunofluorescent channels, and the second column merges the immunofluorescent channels with the phase channel. DAPI in blue (nuclear stain), FITC in green, and mCherry in red. All four rows represent CD68 (FITC) and Perforin (mCherry) double immunofluorescence at different time points in the metrial gland (from top to bottom): GD12, GD16, PPD1, PPD3. Scale bar, 100 um.

Figure 19. Virgin endometrium at 40X magnification. DAPI in blue (nuclear stain), FITC in green, and mCherry in red. First row corresponds to CD68 (FITC)

and Annexin V (mCherry); second row corresponds to CD68 (FITC) and MerTK (mCherry); third row corresponds to CD68 (FITC) and Perforin (mCherry). Scale bar, 50 um.

Figure 20. Double Immunofluorescence for GD12 Decidua (D) and Metrial Gland (MG) at 40X magnification. DAPI in blue (nuclear stain), FITC in green, and mCherry in red. First two rows correspond to CD68 (FITC) and Annexin V (mCherry); third and fourth rows correspond to CD68 (FITC) and MerTK (mCherry); fifth and sixth rows correspond to CD68 (FITC) and Perforin (mCherry). Scale bar, 50 um.

Figure 21. Double Immunofluorescence for GD16 Decidua (D) and Metrial Gland (MG) at 40X magnification. DAPI in blue (nuclear stain), FITC in green, and mCherry in red. First two rows correspond to CD68 (FITC) and Annexin V (mCherry); third and fourth rows correspond to CD68 (FITC) and MerTK (mCherry); fifth and sixth rows correspond to CD68 (FITC) and Perforin (mCherry). Scale bar, 50 um.

Figure 22. Double Immunofluorescence for PPD1 Decidua (D) and Metrial Gland (MG) at 40X magnification. DAPI in blue (nuclear stain), FITC in green, and mCherry in red. First two rows correspond to CD68 (FITC) and Annexin V (mCherry); third and fourth rows correspond to CD68 (FITC) and MerTK (mCherry); fifth and sixth rows correspond to CD68 (FITC) and Perforin (mCherry). Scale bar, 50 um.

Figure 23. Double Immunofluorescence for PPD3 Decidua (D) and Metrial Gland (MG) at 40X magnification. DAPI in blue (nuclear stain), FITC in green, and mCherry in red. First two rows correspond to CD68 (FITC) and Annexin V (mCherry); third and fourth rows correspond to CD68 (FITC) and MerTK (mCherry); fifth and sixth rows correspond to CD68 (FITC) and Perforin (mCherry). Scale bar, 50 um.

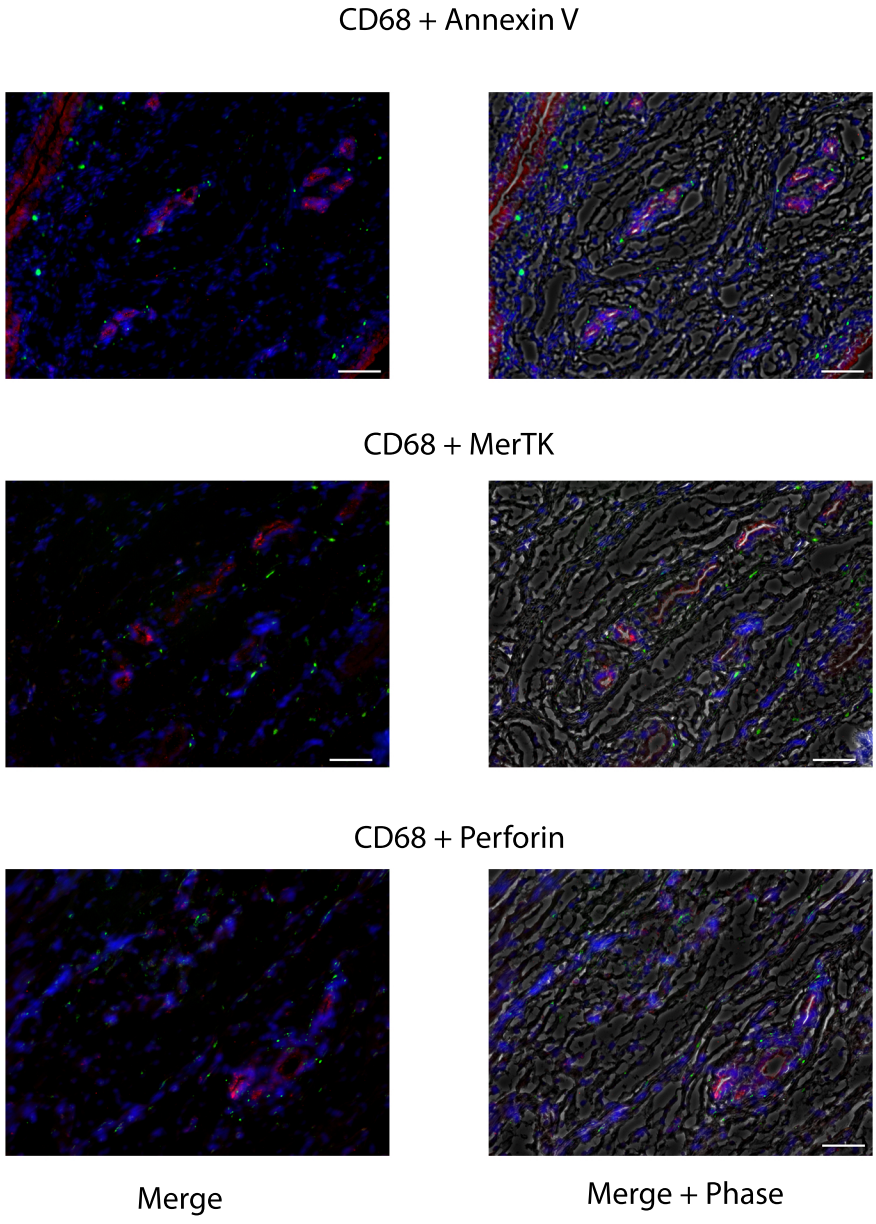

Figure 12. Virgin endometrium at 10X magnification

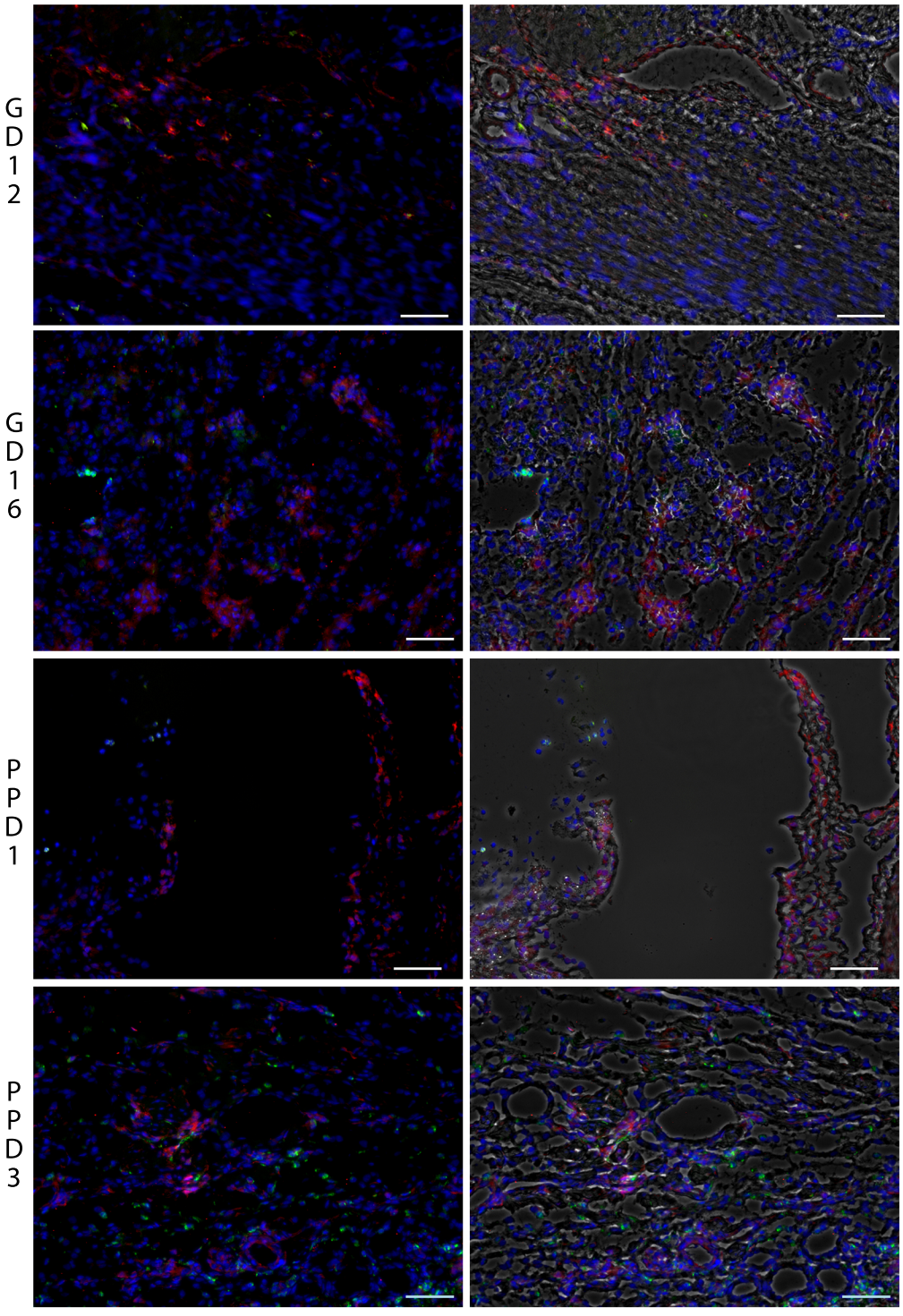

Figure 13. CD68 and Annexin V co-stains in Decidua at 10X magnification

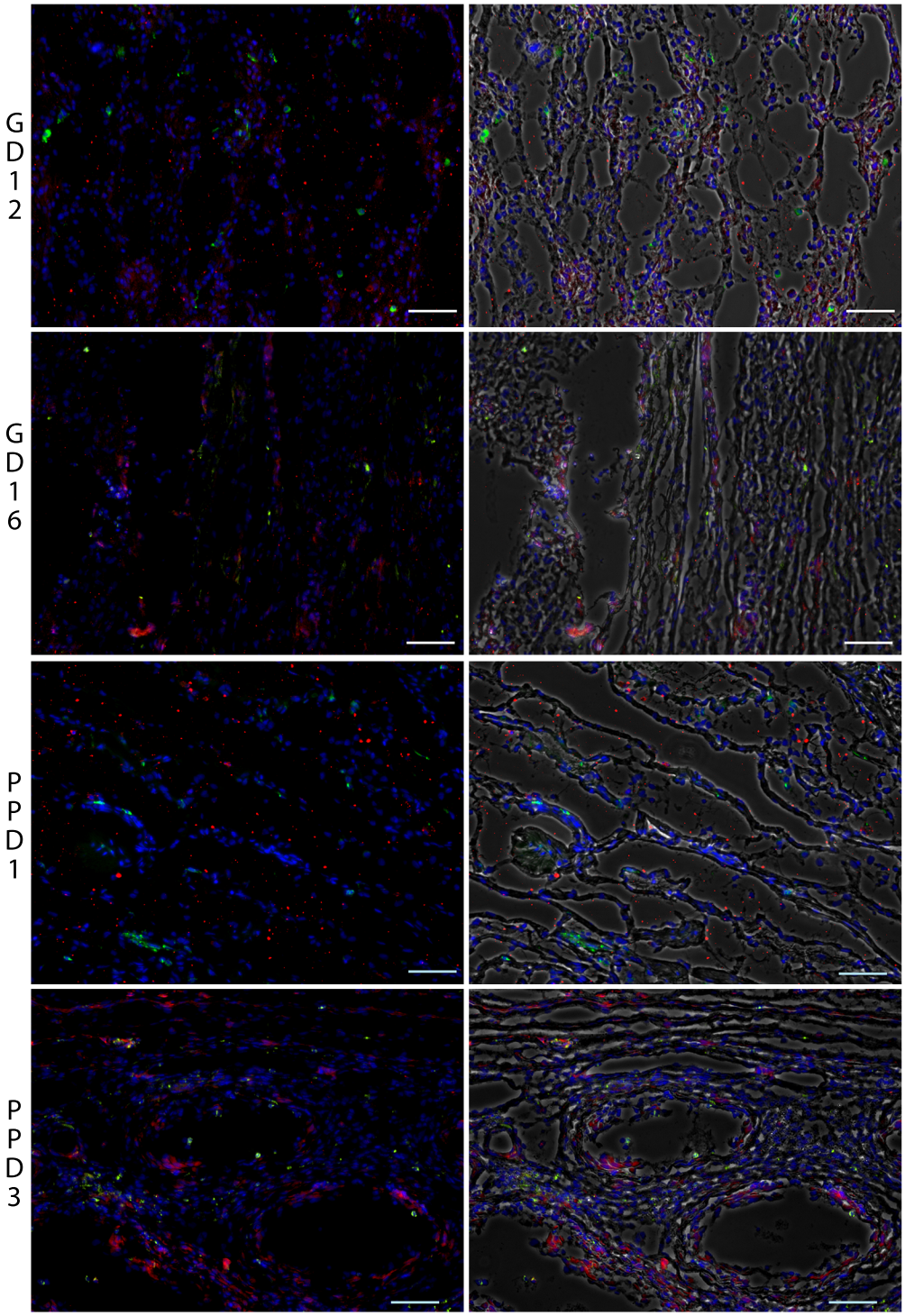

Figure 14. CD68 and Annexin V co-stains in the Metrial Gland at 10X magnification

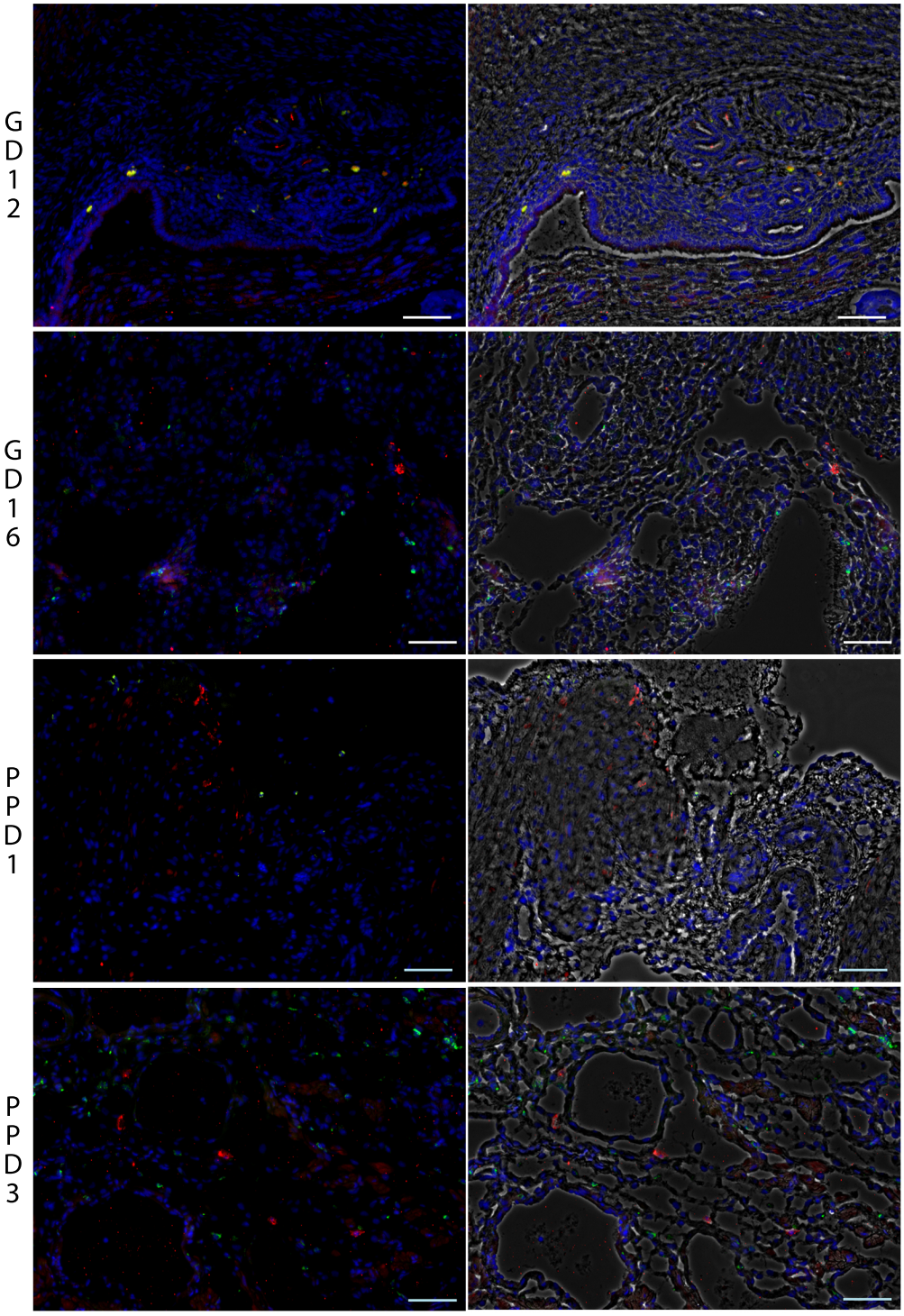

Figure 15. CD68 and MerTK co-stains in Decidua at 10X magnification

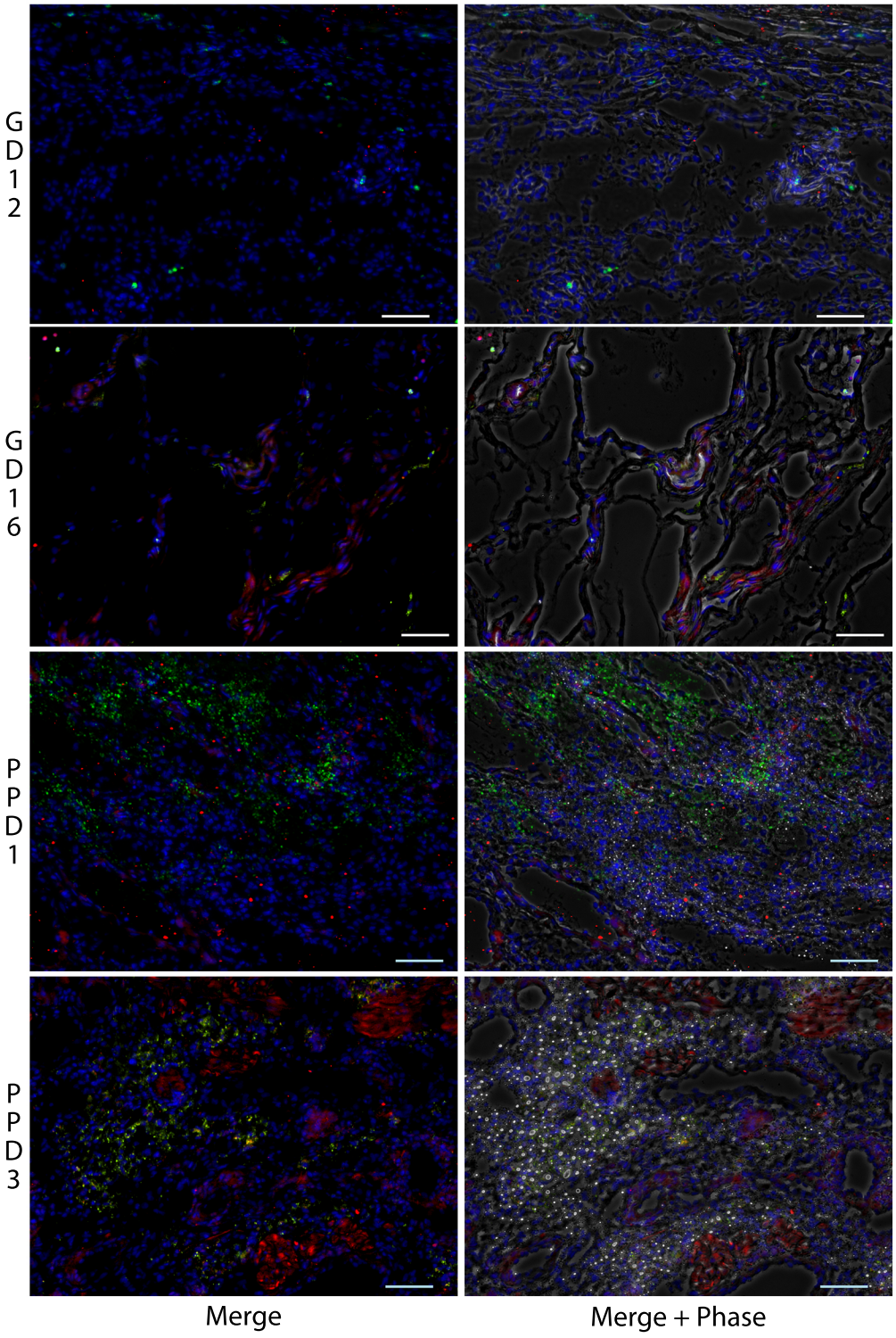

Figure 16. CD68 and MerTK co-stains in Metrial Gland at 10X magnification

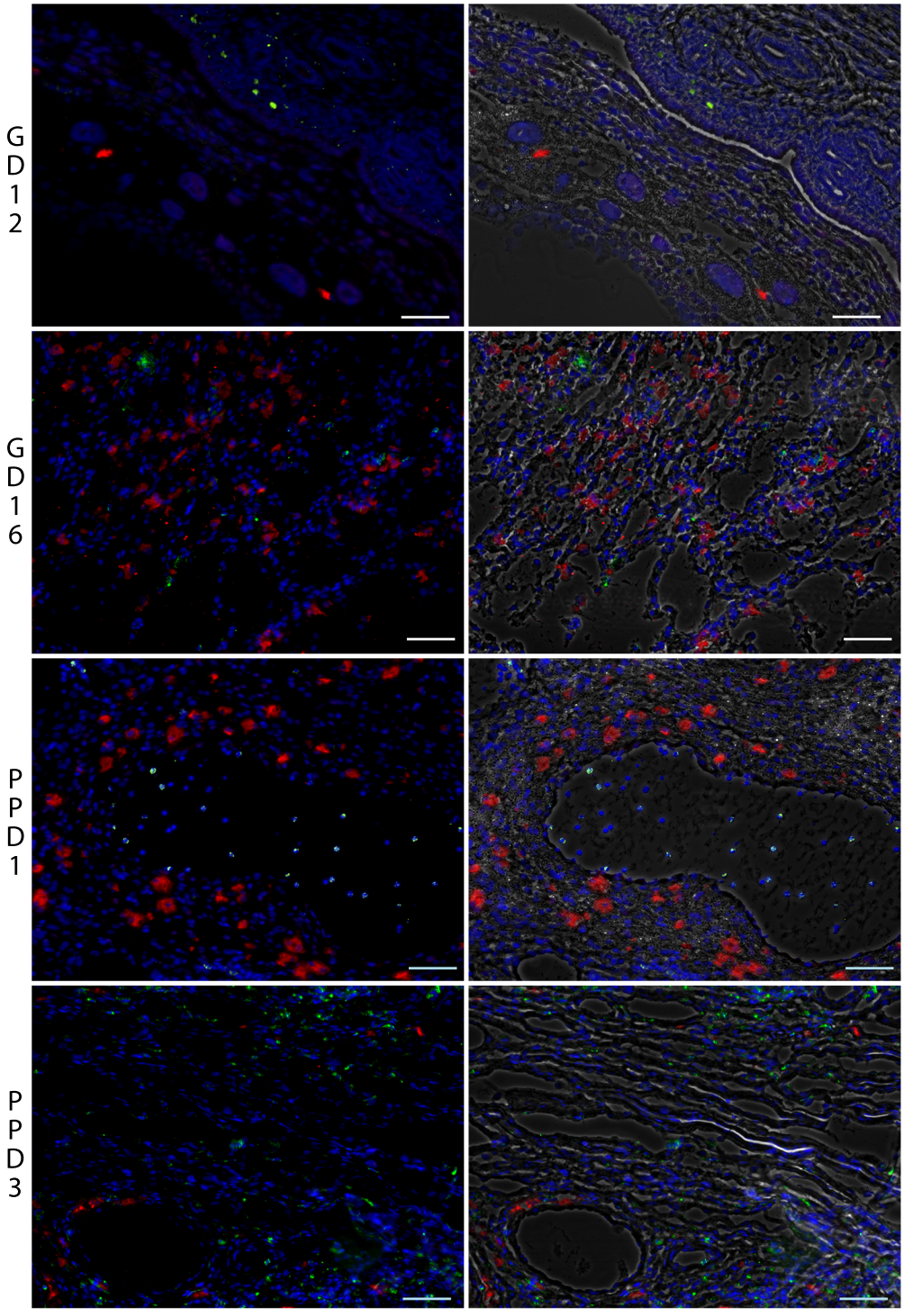

Figure 17. CD68 and Perforin co-stains in Decidua at 10X magnification

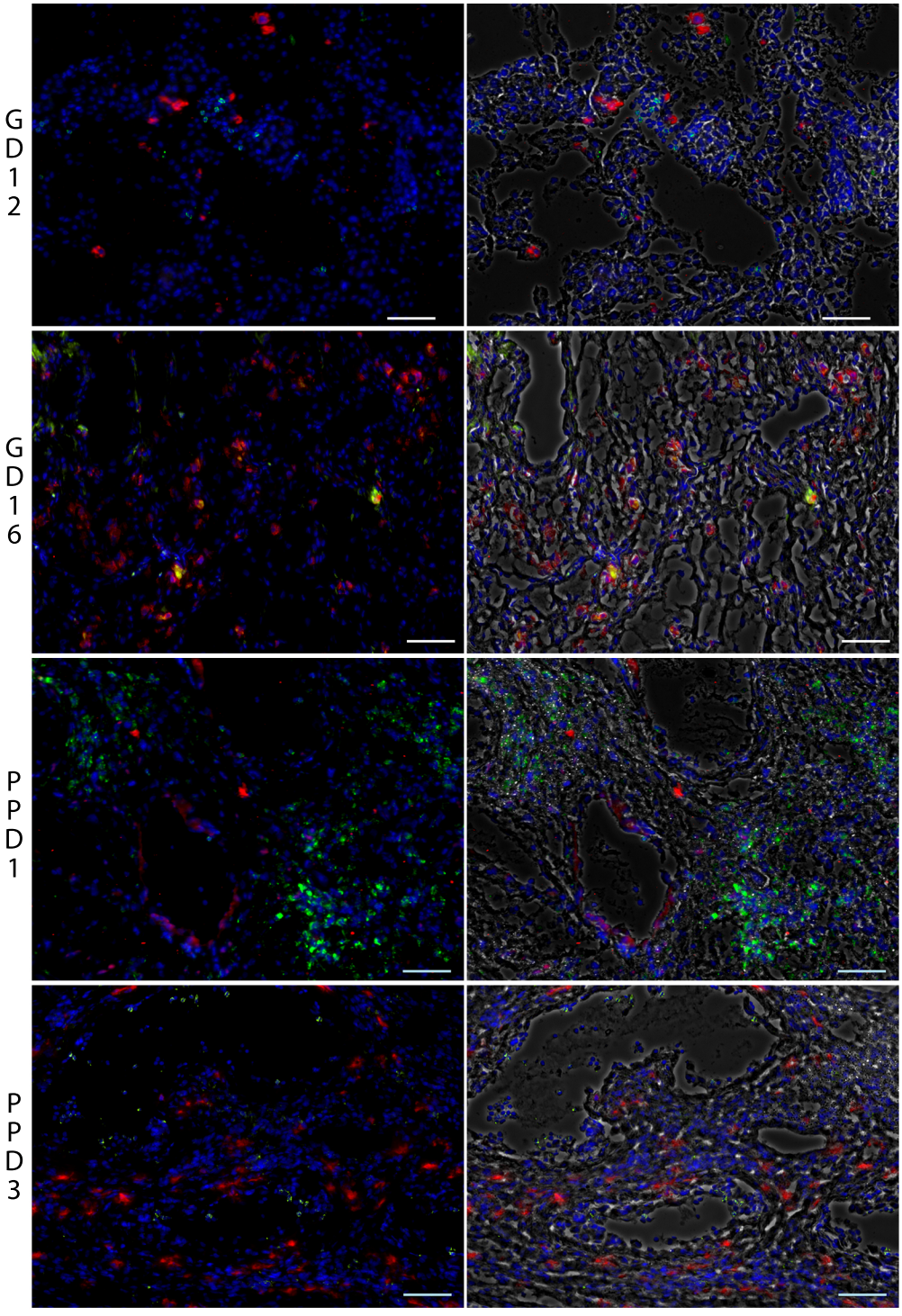

Figure 18. CD68 and Perforin co-stains in Metrial Gland at 10X magnification

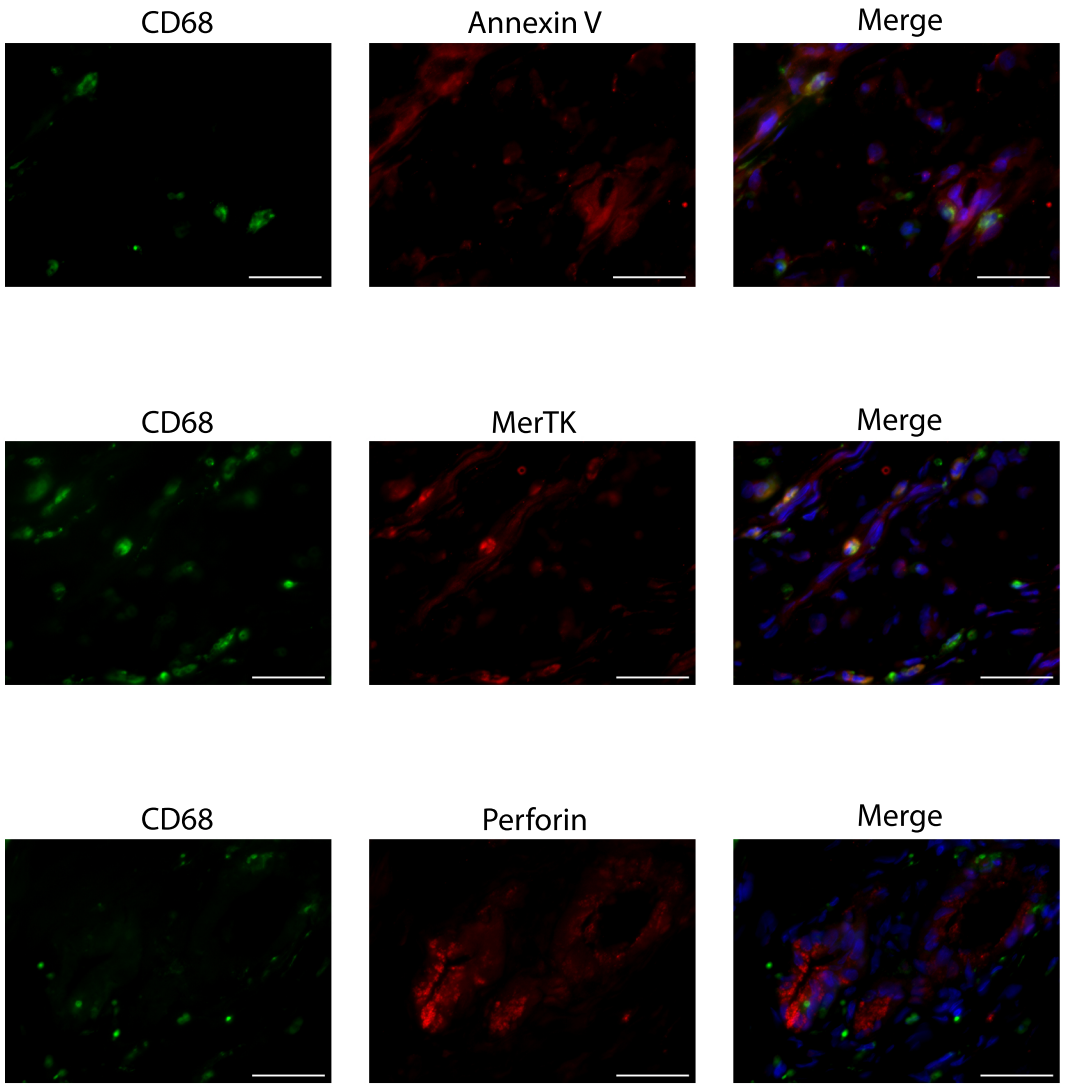

Figure 19. Virgin endometrium at 40X magnification

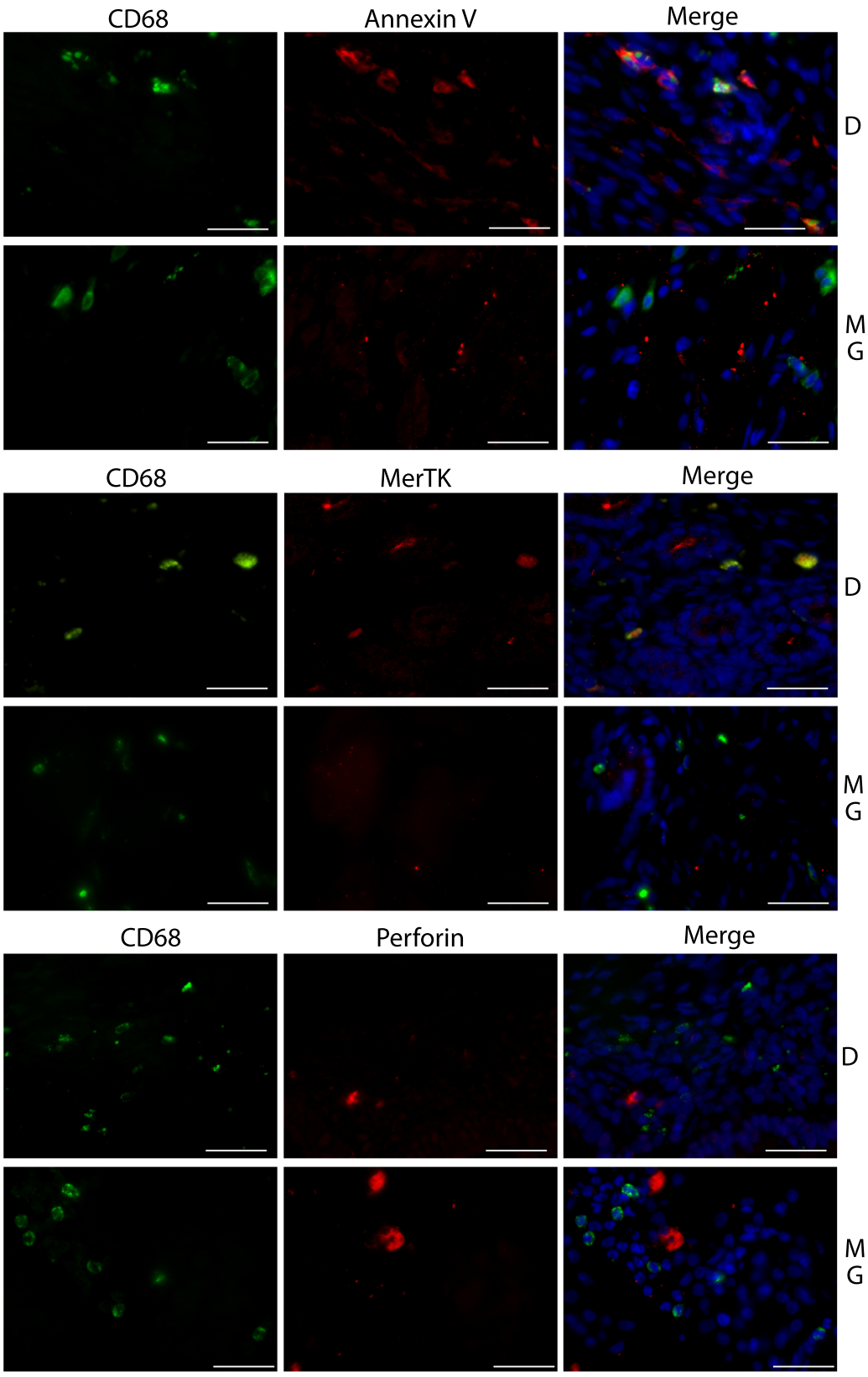

Figure 20. Double Immunofluorecence for GD12 at 40X magnification

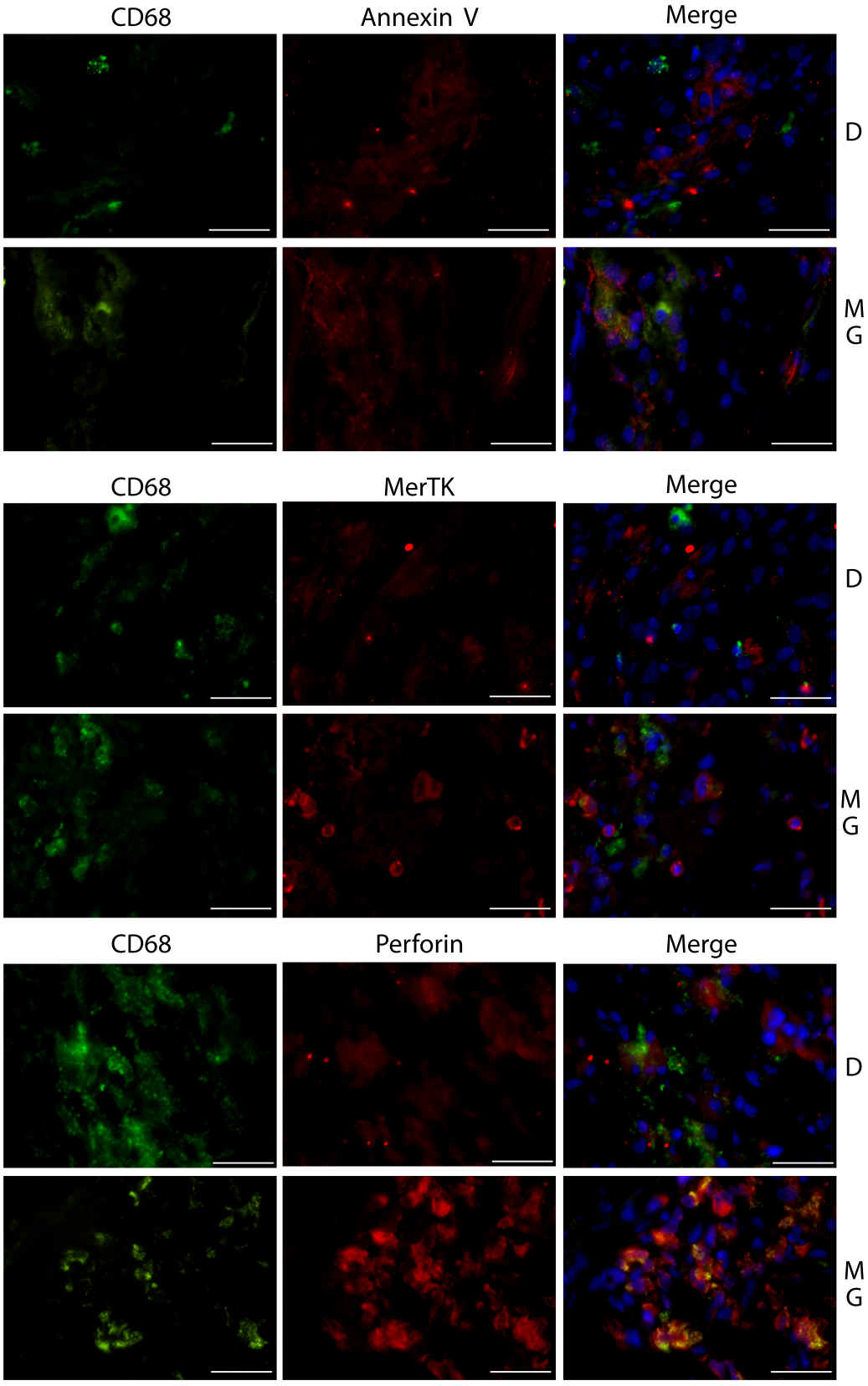

Figure 21. Double Immunofluorescence for GD16 at 40X magnification

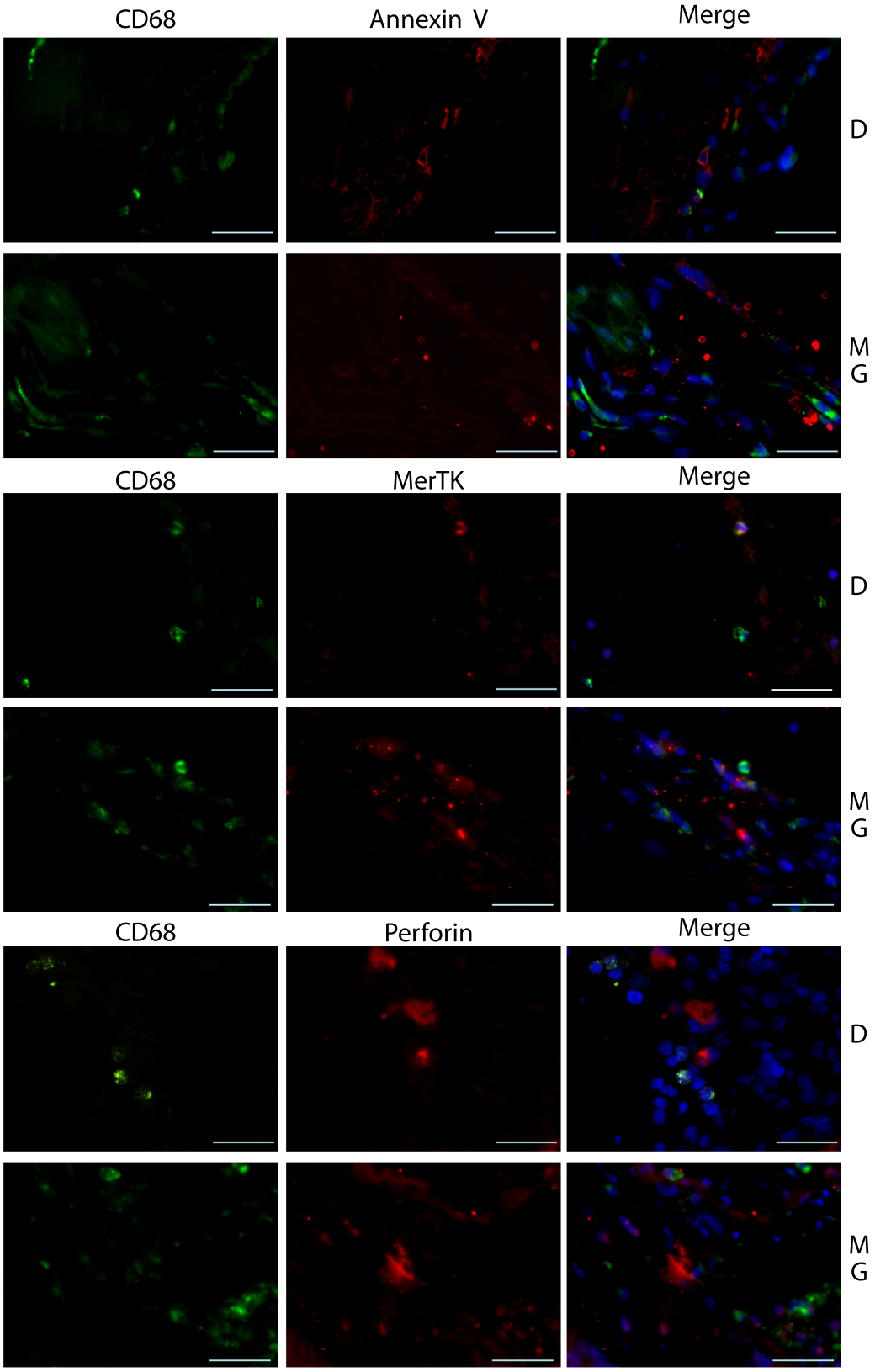

Figure 22. Double Immunofluorescence for PPD1 at 40X magnification

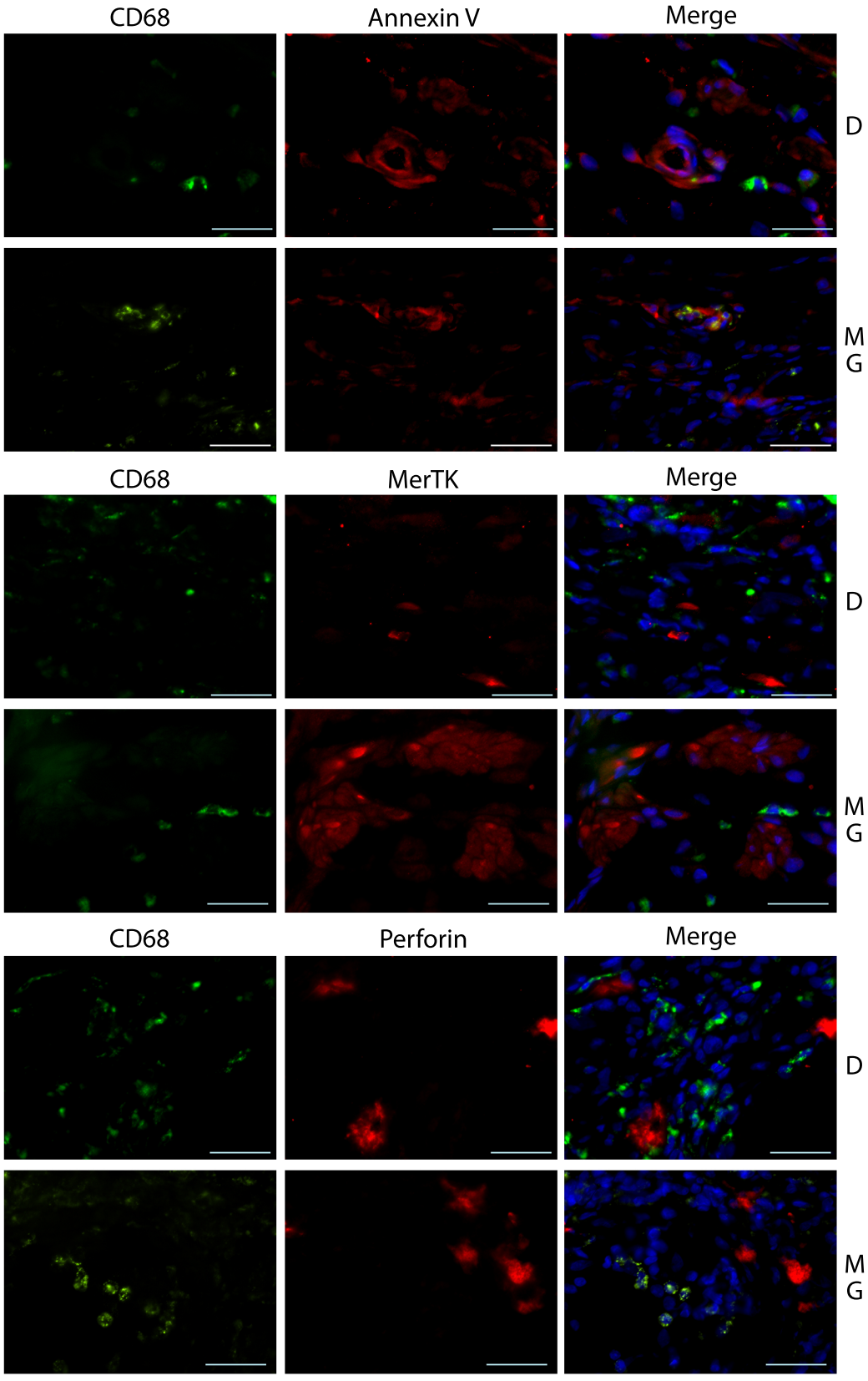

Figure 23. Double Immunofluorescence for PPD3 at 40X magnification

DISCUSSION

Quantitative Real-Time PCR and Immunofluorescence Studies Reveal Insights on Macrophage Function and the Uterine Tissue Microenvironment

In this study, we set out to explore a putative role for macrophages in facilitating spiral artery remodeling during pregnancy, and tissue remodeling during uterine postpartum involution. In sync with the trophic roles that macrophages play in tissue homeostasis and remodeling in a variety of contexts, we would expect that in the context of pregnancy as well that the macrophages would be immunomodulatory when engulfing apoptotic cellular debris. We hypothesized that metrial gland and decidual tissue on days 12, 14, and 16 of pregnancy and postpartum day 3 will be enriched for mRNA transcripts corresponding to anti-inflammatory markers such as TGFβ, phosphatidylserine receptors such as Tim3 and MerTK, and for the pan-macrophage marker CD68, while the mRNA transcripts for pro-inflammatory molecules such as TNFα will be low. The results from quantitative real-time PCR (qPCR) studies were consistent with the hypothesis.

Consistent with the literature, our qPCR results suggested that macrophages are indeed present in the metrial gland and decidual region of the rat uterus, based on the presence of high levels of CD68 mRNA. Were those macrophages participating in cell networks that were generally immunosuppressive, or inflammatory?

Our qPCR data showed that there was higher level of TGFβ mRNA expression in comparison to that of TNFα in the uterine tissue during mid-pregnancy (days 12, 14, and 16) and on postpartum day 3. This suggests that the uterine microenvironment is more immunosuppressive (due to high TGFβ expression) than it is inflammatory (due to low TNFα expression). This appears to be consistent with the existing literature.

For instance, TGFβ isoforms TGFβ1, TGFβ2, and TGFβ3 are expressed at high levels in the decidua basalis on days 14 through 18 and are important in modulating the apoptosis of epithelial cells in the uterus. Moreover, TGFβ1 specifically induces apoptosis in endometrial stromal cells during pregnancy (Shooner et al 2005). Clusters of cells appearing to be macrophages express high levels of TNFα in the uteri of human patients with severe preeclampsia (Pijnenborg et al. 1998). Another study found that elevated levels of TNFα in the placental tissue and in peripheral blood led to increased rates of trophoblast apoptosis in the first trimester of pregnancy and associated with a higher risk of developing preeclampsia later on (Whitley et al. 2007).

Data from qRT-PCR showed that MerTK expression was fairly low during mid-pregnancy time points (days 12, 14, and 16) and was highest in the uterus on postpartum day 3; the only postpartum time point analyzed. This suggested that if MerTK is the molecule important for macrophage-mediated phagocytosis, then macrophages in mid-pregnancy were not involved in efferocytosis of apoptotic cells.

However, immunofluorescence analysis of 6um-thick frozen tissue sections revealed the presence of $MerTK^{+}$ macrophages in the decidual region on gestation day 12, postpartum day 1, and in the virgin uterus. Macrophages in the decidua on gestation day 16 and postpartum day 3, and all of the time points in the metrial gland, appeared to not have MerTK-positive macrophages. Moreover, the number of macrophages that were MerTK-positive in the decidua were very low in number compared to MerTK-negative macrophages.

It appeared that MerTK is more highly expressed in postpartum, and less abundantly during mid-pregnancy as illustrated by qRT-PCR. But by immunofluorescence, it colocalized with CD68 on a small subset of cells, and in many instances was expressed on unknown cells in both the decidua and the metrial gland. These unidentified cell types morphologically resembled endothelial cells due to the way they were arranged in a circular pattern around what appeared to be the lumen of blood vessels. But to confirm this, it would be important to stain for the endothelial cell marker PECAM-1 in the future. If these MerTK-positive cell types were endothelial or epithelial cells, this would not be very surprising since ‘Mer’ refers to ‘myeloid-epithelial-reproductive’ receptor tyrosine kinase.

CD68 and Annexin V double immunofluorescence stainings in both the decidua and metrial gland did show spatial proximity between macrophages and apoptotic cells suggesting that macrophages might be important for the engulfment of apoptotic cells during pregnancy (on days 12, 14, and 16) and

postpartum (on days 1 and 3). These data suggest that another phagocytic receptor besides MerTK might also be important for macrophage-mediated phagocytosis in the MerTK-negative macrophage subsets.

Lastly, we assessed the presence of natural killer (NK) cells, which could work cooperatively with macrophages in remodeling. CD68 and Perforin double immunofluorescence stainings suggested that macrophages and NK cells were both present in the decidua and metrial gland in various patterns. During mid-pregnancy (days 12, 14, and 16) it appeared that NK cells were present in a higher proportion compared to macrophages, while during the postpartum period, macrophages seemed to be higher in number, especially on the edges of the metrial gland region. There was also a trend of macrophages appearing to be present in the lumen of blood vessel-like structures, while NK cells were found interspersed in the decidual and metrial gland parenchyma.

Out of all images examined, only in the metrial gland on day 16 did it appear as if there was some cross-talk occurring between macrophages and NK cells due to the almost overlapping levels of spatial proximity between the two cell types. In the future, it would be important to quantify the relative numbers of these two cell types, and also ascertain if there are any other regions or time points where the two cell types appear to be spatially close.

Hypothesized Model Supported By the Data

It has been already established that NK cells take part in the first wave of uterine spiral artery remodeling starting around gestation day 6.5 (Soares et al.

2012). In the second wave of remodeling beginning around gestation day 10.5, invasive trophoblasts begin to migrate towards the myometrium (Robson et al. 2012). Existing reports suggest that some of these trophoblast cells undergo apoptosis as they migrate, in addition to more importantly facilitating the apoptosis of vascular cells (endothelial and smooth muscle) in the decidual region (Whitley and Cartwright 2009).

The low levels of TNFα and high levels of TGFβ expression might have a role to play in inducing the expression of MerTK, since this has been reported in other biological contexts. For instance, in a cell culture model of multiple sclerosis, microglia cells that were treated with the isoform TGFβ1 were found to upregulate MerTK expression and phagocytize myelin present on nearby co-cultured neurons (Healy et al. 2016). While detrimental in the case of myelin phagocytosis, TGFβ1-mediated upregulation of MerTK might be an efficient strategy to increase phagocytosis of cellular debris in the context of pregnancy, since high TGFβ levels might also help suppress inflammation.

Our data illustrates that some apoptotic cells (marked by Annexin V) are present in the decidual and metrial gland regions in proximity to macrophages. However, MerTK-positive macrophages were only detectable in the decidua. This suggests that invasive fetal trophoblasts and maternal cells that undergo apoptosis in the maternal decidua might be getting engulfed by MerTK-expressing macrophages. Contrastingly, in the metrial gland region that lies deeper in the placental bed, macrophages either might not be engulfing apoptotic cells, or might

be using a molecule other than MerTK for efferocytosis. Alternatively, it is plausible that high rates of apoptosis might be occurring much earlier during gestation in the metrial gland, leading to lower detection of Annexin V^+ apoptotic cells and lack of MerTK-positive macrophages in the metrial gland region.

Based on the established literature and the data that we collected, we suggest the following model of apoptotic cell clearance with macrophages as the key cell type (figure 24). NK cells initiate spiral artery remodeling by inducing apoptosis in endothelial and vascular smooth muscle cells of arteries being remodeled (Robson et al. 2012). They then help modulate the rate at which endovascular and interstitial trophoblasts invade towards the maternal myometrium. While apoptosis is occurring in both maternal and fetal cells, our data suggest that anti-inflammatory molecules, such as TGFβ, are being secreted by various cell types to polarize the macrophages to express phosphatidylserine receptors such as MerTK that help them engulf nearby apoptotic cells without causing inflammation. A similar mechanism of apoptotic cell clearance might also play out during postpartum involution.

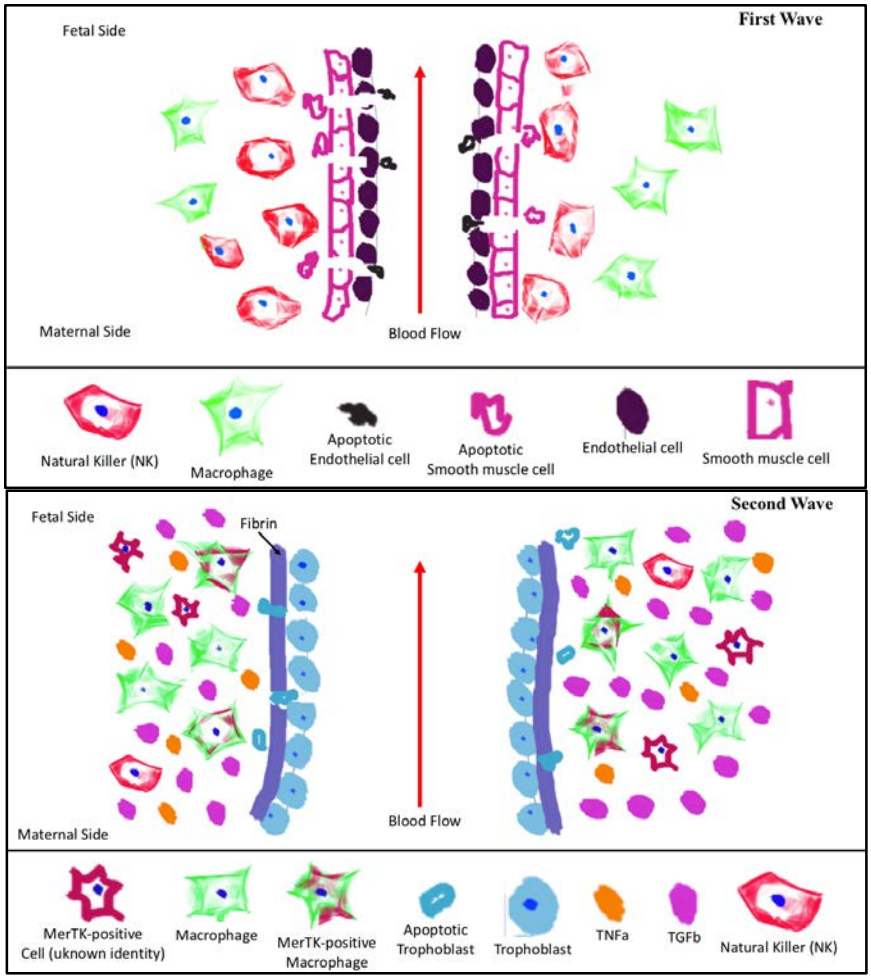

Figure 24: Hypothesized model of spiral artery remodeling based on the established literature and the insights gained from our data. Spiral artery remodeling proceeds in two waves, where the first wave is initiated by uterine natural killer cells and the second wave is led by trophoblast invasion (Soares et al. 2012). Remodeled arteries (bottom image) are much more dilated than their non-remodeled counterparts (top image). They lose smooth muscle, and instead become associated with trophoblasts and coated with a layer of fibrin, a form of connective tissue (Burton et al. 2009). Invasive trophoblasts also undergo apoptosis during their migration towards the uterine wall (Mor and Abrahams 2004). Hence, during both waves, maternal and fetal apoptotic cells abound in the placental bed. It is already known that macrophages are present in the tissue during this time (Faas and de Vos 2017). Our data shows that these macrophages are in proximity to apoptotic cells, and that the uterine tissue microenvironment is immunosuppressive given the high TGFβ levels in contrast to the low TNFα levels. Our results also suggest that a small subset of macrophages express a phosphatidylserine receptor called MerTK, which might be relevant to macrophage-mediated clearance of apoptotic cellular debris.

Limitations of the Data

One of the main limitations of our data were that some immunofluorescence stainings for MerTK and Annexin V did not show clear signal. For instance, it was difficult to distinguish between nonspecific binding of the antibody to the tissue, and specific binding of the antibody to the antigen. This required us to make digital corrections of the image histogram for each of the images. However, for consistency of analysis, the corrections were carried out for all sections imaged for any particular antibody.

Another limitation of the data might be the antibody that was chosen to recognize MerTK. MerTK is phosphorylated in macrophages that carry out MerTK-mediated phagocytosis of apoptotic cells. Hence, an antibody specific to phosphorylated MerTK should have been chosen for the CD68 and MerTK double immunofluorescence staining. This might have improved the signal-to-noise ratio of the images.

Lastly, to obtain tissue sections that better preserve the morphology of the tissue being examined, it would be useful to embed tissue blocks in paraffin prior to sectioning and staining (which can then easily be deparaffinized during staining using standard protocols). Alternatively, if using frozen OCT-embedded sections, it would be important to fix tissues right after dissection and dehydrate them using a sucrose gradient prior to embedding in OCT as another way of preserving some of the morphology, if the paraffin method is harder to carry out. Better morphological information would help us make better claims about the tissue

architecture in which different cell types are residing and carrying out important functions.

Other Molecules Should be Studied to Further Understand Maternal Macrophage Function

In this study, we focused our attention solely on a single phosphatidylserine receptor MerTK, whose expression pattern resembled that of CD68, unlike Tim3, which during preliminary experiments followed an mRNA expression pattern different from that of the macrophage marker CD68. We also made this decision based on the idea that Tim3 expression wasn't highly specific to macrophages, since other myeloid (NK and dendritic cells) and lymphoid (T) cell subsets expressed Tim3. However, it will be important to re-evaluate the importance of this receptor in the context of pregnancy since some studies have revealed that blocking Tim3 expression in macrophages can lead to accumulation of apoptotic cells (Han et al. 2013). Hence, even though MerTK or another unknown phosphatidylserine receptor might be more specific to macrophages and easier to target macrophage function therapeutically, Tim3 still needs further study. It will also be important to look at the expression and localization of another Tim protein family member: Tim4, which in other biological contexts has been shown to facilitate engulfment of apoptotic cells by macrophages (Nishi et al. 2014).

Besides the TIM family, another well-known biomolecule worthy of pursuit is Milk fat globule-epidermal growth factor-factor 8 (Mfge8), more

commonly called Lactadherin. Lactadherin is a peripheral membrane glycoprotein which has been studied in the context of many diseases such as systemic lupus erythematosus, wound healing, and tumor angiogenesis (Kaminska et al. 2017). In efferocytosis, lactadherin acts as a bridging molecule to facilitate engulfment of an apoptotic cell. First, macrophages secrete lactadherin that binds to exposed phosphatidylserine on the surface of apoptotic cells. Lactadherin then tethers the apoptotic cell to the macrophage. This in turn triggers the macrophage to "develop" or get activated to engulf the dying cell. Lactadherin has been shown to be expressed by many macrophage subsets including microglia in the brain (Fuller et al. 2008). Hence, it would be interesting to study whether this molecule plays a functionally-relevant role in the removal of apoptotic cells during pregnancy.

In addition to studying macrophage-associated markers, it would be important to look more closely at markers of NK, trophoblast, endothelial, and smooth muscle cells both by qRT-PCR and immunofluorescence and carry out different combinations of double or triple marker immunofluorescence staining to investigate whether two biomarkers colocalize to the same cell, or if there is any proximity between two different cell types.

For instance, we observed that macrophages and perforin-positive NK cells were close to each other in the metrial gland on gestation day 16, which suggests that they might be interacting. Hence, it might be possible that other cell types such as macrophages and trophoblasts are spatially close as well. Or to

identify the MerTK-positive cells of unknown identity, which morphologically resembled endothelial cells, it would be important to carry out double immunofluorescence staining for MerTK and the endothelial cell marker PECAM-1.

Broader Implications of Studying Macrophage-Mediated Uterine Remodeling

In this study, we investigated the role of macrophages in spiral artery remodeling during a healthy rat pregnancy. But are the plausible functions carried out by macrophages in pregnancy relevant to what is known about their role in other areas of health and disease? It turns out that macrophages perform similar functions, such as immunomodulation, tissue homeostasis, and remodeling in a wide variety of contexts. This makes them important players in different pathogenic states such as preeclampsia-associated cardiovascular abnormalities, myocardial infarction, vertical transmission of Zika virus, and tumorigenesis.

The Link Between Preeclampsia and Cardiovascular Disease

It is important to understand how macrophages and other immune cell populations contribute to preeclampsia in order to derive insights into what these cells might be doing in the context of cardiovascular disease. The rat model of spiral artery remodeling can be useful to study this. Many studies have shown that preeclamptic women have higher rates of developing cardiovascular disease in the long term (Valdes 2017).

Two probable mechanisms have been proposed in the literature. First, it appears that preeclampsia and cardiovascular disease have many common risk factors, which can get triggered due to the stress experienced during pregnancy. In a way, a preeclamptic pregnancy paves the way for future cardiovascular pathologies. The three-step model of preeclampsia posits that: during stage 1, misregulated immunological function leads to aberrant placental development; leading to stage 2, where there is decreased trophoblast invasion and reduced remodeling of spiral arteries; finally resulting in stage 3, where oxidative stress factors and other signals emanating from aberrantly remodeled spiral arteries circulate in the maternal bloodstream leading to systemic endothelial cell dysfunction, proteinuria, hypertension among others (Staff et al. 2010).

Alternatively, preeclampsia and cardiovascular disease might be linked by lipid deposition as well. Maternal hyperlipidemia is a common occurrence prior to a preeclamptic pregnancy. The “acute atherosis” of preeclamptic spiral arteries is described to be a result of subendothelial lipid-filled foam cells (identified to be CD68-positive macrophages), vascular (fibrinoid) necrosis (perhaps due to elevated levels of TNFα), and perivascular lymphocytic infiltration. Similar characteristics such as increased uptake of oxidized LDLs, increased levels of proinflammatory cytokines TNFα and IL-6 have been shown to be involved in atherosclerosis and coronary heart disease as well (Staff et al. 2010). Interestingly, macrophages themselves can also accumulate cholesterol and be found in atherosclerotic lesions (Moore et al. 2013).

Our study on the trophic roles played by macrophages during pregnancy has direct implications for understanding how preeclampsia develops. In future studies, we can use our system to develop a preeclamptic rat model by way of making trophoblasts defective in migration. For instance, by knocking down the gene TET1 that is implicated in trophoblast migration (Zhu et al. 2017), we could make the second-wave of spiral artery remodeling defective. We could then test to see if this phenotype can be "cured" by over-expressing phosphatidylserine receptors or apoptosis-inducing cytokines in macrophages that could then assist in the proper remodeling of the spiral arteries regardless of trophoblast invasion. We could also use this proposed preeclamptic rat model to carry out a longitudinal investigation of cardiovascular disease in the preeclamptic rat post-pregnancy, and characterize the phenotype displayed by the macrophages.

Efferocytic Molecules are Important for Post-Infarction Cardiac Repair

The study of spiral artery remodeling and postpartum uterine repair can be influenced by, and can in turn influence, the understanding of how the tissue in the heart is repaired after a myocardial infarction (colloquially termed as a "heart attack"). A myocardial infarction results in the death of many cardiomyocytes (heart muscle cells), which if not removed in a timely manner from the tissue, can lead to tissue inflammation, thereby slowing down the growth of new cardiomyocytes and delaying cardiac repair. This context of unresolved inflammation resembles that seen during aberrant spiral artery remodeling in cases such as preeclampsia.

A recent study found that MerTK and Mfge8 (Lactadherin) help in the efficient and timely phagocytosis of apoptotic cardiomyocytes after a myocardial infarction. The timely removal of apoptotic cardiomyocytes is important to facilitate repair of the injured cardiac tissue. Failure to remove the apoptotic cells implies that the tissue will remain inflamed for a longer period of time, leading to a higher risk of heart failure. The study showed that bone-marrow derived Ly6C-expressing monocytes/macrophage populations that expressed both MerTK and Mfge8 were the most efficient at synergistically engulfing apoptotic cardiomyocytes, and their activation lead to the secretion of VEGFA in the tissue to allow inflammation to resolve more quickly.

Based on these studies, it would be interesting to test the expression levels of lactadherin in uterine tissue during pregnancy and postpartum using qRT-PCR, flow cytometry and/or immunofluorescence. If lactadherin is expressed on macrophages in the decidua and metrial gland, then this may suggest a similarity between the mechanisms of efferocytosis used during cardiac repair after a myocardial infarction and spiral artery remodeling during pregnancy.

Transmission of Zika Virus from the Mother to the Fetus Might be Facilitated by Pregnancy-Associated Macrophages

Our model of spiral artery remodeling can be modified to better understand the pathogenesis of Zika virus infection. Mechanism of vertical intrauterine transmission of Zika virus from mother to fetus is an area of active research. Recent studies have shown that Zika virus (ZIKV strain PRVABC59

(PR 2015)) infects and replicates in placental macrophages, called Hofbauer cells, and also in cytotrophoblasts, based on samples isolated from villous tissue of full-term human placentae.

Mouse models also suggest that ZIKV infects placental macrophages, which can then act as carriers for disseminating the virus to other fetal cells by facilitating physical disruption of the placental barrier. Earlier studies had hinted that members of the tyrosine kinase family Tyro3, Axl, or MerTK (TAMs) might be important for infection of cells by the Zika virus, but a recent study showed that in a mouse knockout model of TAMs, viral infection and replication still occurred. This leaves an open question as to how Hofbauer and cytotrophoblast cells get infected and how therapies can be developed to block the transmission of the virus from the mother to the fetus.

Recently, a rat model of perinatal Zika virus infection was developed in a lab to study the infectivity and viral clearance in dams and their pups (Sherer et al. 2017). Hence, our model of the rat can also be modified to study Zika virus transmission from mother to fetus. In the future, we could use clodronate liposomes to deplete macrophages from the uterus and then check whether Zika is still transmitted to the fetus. Alternatively, we could inject the rat with antibodies targeting different macrophage receptors to finally identify the mode through which vertical transmission of the virus occurs. We could also study whether macrophages infected by the Zika virus are unable to perform functions such as phagocytosis.

Besides focussing just on macrophages, we could also investigate the role of NK cells in Zika virus transmission. This is because NK cells are an innate immune cell type that possess the ability to identify other cells that have been infected with a virus. Hence, strategies could be developed to use NK cells as a "therapeutic" that targets macrophages that have been infected by Zika.

Functional Attributes of Macrophages in the Uterine Microenvironment May Provide Insights Into their Role in Tumorigenesis

The rat model of spiral artery remodeling and postpartum uterine repair can be used to discover macrophage-associated molecules that are implicated in apoptotic cell clearance, angiogenesis, immunosuppression, and other phenomena that occurs during tumor progression. Tumor-associated macrophages, also called the TAMs, are an area of active research. They have been shown to originate from a bone marrow-derived myeloid precursor population and shown to facilitate cancer metastasis by stimulating tumor angiogenesis and inhibiting T-cell-initiated antitumor immune responses.

A recent study showed that MerTK can be therapeutically targeted on tumor macrophages to prevent cancer relapse after radiation therapy (Crittenden et al. 2016). TNFα can regulate expression of PD-L1 on murine tumor-associated monocytes and macrophages (Hartley et al. 2017). Myeloid cell-specific TGFβ signaling can promote cancer metastasis (Pang et al. 2013). Prostate-cancer associated macrophages become polarized in the presence of apoptotic cancer cells and hence get induced to express Mfge8 at high levels (Soki et al. 2014).

Similarly, Tim3 expression has been linked to progression of hepatocellular carcinoma and reduced patient survival (Flecken and Sarobe 2015).

These studies, among numerous others provide ample evidence that macrophages of an “alternative” or “M2” phenotype are usually detrimental in the context of cancer. However, M2-like macrophages appear to be a healthy component of tissue remodeling during pregnancy and postpartum. This again reinforces the importance of the idea that studying macrophage function in pregnancy can reveal new insights into macrophage function in tumorigenesis.

Since myeloid cells such as macrophages can suppress T cell function against tumor cells (Gabrilovich and Nagaraj 2009), we could focus our future studies on how macrophages signal to other immune cell types such as NK cells and T cells during pregnancy. We have already observed possible interactions between macrophages and NK cells on gestation day (GD) 16 in the metrial gland. By also staining for T cells, we could identify interactions between macrophages and T cells in the context of pregnancy-associated remodeling, and later try to extrapolate that to what macrophages might be doing in the tumor microenvironment.

CONCLUSION

In this study, we investigated the role of macrophages in apoptotic cell clearance during pregnancy and postpartum in a rat model system. We used qRT-PCR and double immunofluorescence studies to identify genes being expressed by macrophages and whether macrophages were expressing markers that correlated with an efferocytic function. Our data suggested that macrophages were spatially proximal to apoptotic cells and that a small subset of macrophages expressed the phosphatidylserine receptor MerTK, which is consistent with an efferocytic role for macrophages.

It is still an open question as to what efferocytic molecules might be expressed by the macrophages that were MerTK-negative. Hence, future studies should explore other phosphatidylserine receptors. The relevance of the macrophage to both the innate and adaptive arms of the immune system make it an important player during gestation and beyond.

Besides having a role in pregnancy-associated tissue remodeling, macrophages have been found to play important functions in other health settings such as cardiac repair, Zika virus transmission, cardiovascular disease, and tumor progression. It will be important to design ways of using the rat model system of studying macrophages in pregnancy to uncover insights into what macrophages might be doing in other biological contexts, and vice-versa.

REFERENCES

1. Perez-Sepulveda A, Torres MJ, Khoury M, Illanes SE. (2014) Innate immune system and preeclampsia. *Frontiers in immunology*. 5-244
2. Sharma, S. (2014) Natural killer cells and regulatory T cells in early pregnancy loss. *The International Journal of Developmental Biology*. **58**, 219–229
3. Guerin, L. R., Prins, J. R., and Robertson, S. A. (2009) Regulatory T-cells and immune tolerance in pregnancy: a new target for infertility treatment? *Human Reproduction Update*. **15**, 517–535
4. Fang, W.-N., Shi, M., Meng, C.-Y., Li, D.-D., and Peng, J.-P. (2016) The Balance between Conventional DCs and Plasmacytoid DCs Is Pivotal for Immunological Tolerance during Pregnancy in the Mouse. *Scientific Reports*. 10.1038/srep26984
5. Muzzio, D. C. A., Zenclussen, A. C., and Jensen, F. (2013) The Role of B Cells in Pregnancy: the Good and the Bad. *American Journal of Reproductive Immunology*. **69**, 408–412
6. Faas, M. M., and Vos, P. D. (2017) Uterine NK cells and macrophages in pregnancy. *Placenta*. **56**, 44–52
7. Ning, F., Liu, H., and Lash, G. E. (2016) The Role of Decidual Macrophages During Normal and Pathological Pregnancy. *American Journal of Reproductive Immunology*. **75**, 298–309
8. Geissmann F, Mass E.(2015) A stratified myeloid system, the challenge of understanding macrophage diversity. *Seminars in Immunology*. ;**27**(6):353–356.
9. Garceau V, Balic A, Garcia-Morales C, Sauter KA, Mcgrew MJ, Smith J, Vervelde L, Sherman A, Fuller TE, Oliphant T, et al. (2015) The development and maintenance of the mononuclear phagocyte system of the chick is controlled by signals from the macrophage colony-stimulating factor receptor. *BMC Biology*. **13**(1):12.
10. Mathias JR, Dodd ME, Walters KB, Yoo SK, Ranheim EA, Huttenlocher A. (2009) Characterization of zebrafish larval inflammatory macrophages. *Developmental & Comparative Immunology*. **33**(11):1212–1217
11. Burton, G., Woods, A., Jauniaux, E., and Kingdom, J. (2009) Rheological and Physiological Consequences of Conversion of the Maternal Spiral Arteries for Uteroplacental Blood Flow during Human Pregnancy. *Placenta*. 30, 473–482
12. Soares, M. J., Chakraborty, D., Rumi, M. A. K., Konno, T., & Renaud, S. J. (2012). Investigating the Hemochorial Maternal-Fetal. *Placenta*, *33*(4), 233–243.
13. Hsu, K.-F., Pan, H.-A., Hsu, Y.-Y., Wu, C.-M., Chung, W.-J., and Huang, S.-C. (2014) Enhanced myometrial autophagy in postpartum uterine involution. *Taiwanese Journal of Obstetrics and Gynecology*. 53, 293–302

14. Smith SD, Dunk CE, Aplin JD, Harris LK, Jones RL. (2009) Evidence for immune cell involvement in decidual spiral arteriole remodeling in early human pregnancy. *American Journal of Pathology*. 174(5):1959-1971
15. Croy, B. A., Chen, Z., Hofmann, A. P., Lord, E. M., Sedlacek, A. L., and Gerber, S. A. (2012) Imaging of Vascular Development in Early Mouse Decidua and Its Association with Leukocytes and Trophoblasts. *Biology of Reproduction*. 87-125
16. Picut, C. A., Swanson, C. L., Parker, R. F., Scully, K. L., and Parker, G. A. (2009) The Metrial Gland in the Rat and Its Similarities to Granular Cell Tumors. *Toxicologic Pathology*. 37, 474–480
17. Furukawa, S., Hayashi, S., Usuda, K., Abe, M., Hagio, S., and Ogawa, I. (2011) Toxicological Pathology in the Rat Placenta. *Journal of Toxicologic Pathology*. 24, 95–111
18. Peel, S., and Stewart, I. (1979) Ultrastructural changes in the rat metrial gland in the latter half of pregnancy. *Anatomy and Embryology*. 155, 209–219
19. Kyathanahalli, C., Marks, J., Nye, K., Lao, B., Albrecht, E. D., Aberdeen, G. W., Nathanielsz, P. W., Jeyasuria, P., and Condon, J. C. (2013) Cross-Species Withdrawal of MCL1 Facilitates Postpartum Uterine Involution in Both the Mouse and Baboon. *Endocrinology*. 154, 4873–4884
20. Aschkenazi, S., Straszewski, S., Verwer, K. M., Foellmer, H., Rutherford, T., and Mor, G. (2002) Differential Regulation and Function of the Fas/Fas Ligand System in Human Trophoblast Cells. *Biology of Reproduction*. 66, 1853–1861
21. Li Y-H, Zhou W-H, Tao Y, Wang S-C, Jiang Y-L, Zhang D, Piao H-L, Fu Q, Li D-J, Du M-R. (2016) The Galectin-9/Tim-3 pathway is involved in the regulation of NK cell function at the maternal–fetal interface in early pregnancy. *Cellular and Molecular Immunology*. 13(1):73–81.
22. Han G, Chen G, Shen B, Li Y. (2013) Tim-3: An Activation Marker and Activation Limiter of Innate Immune Cells. *Frontiers in Immunology*. 4(1)
23. Toda S, Segawa K, Nagata S. MerTK-mediated engulfment of pyrenocytes by central macrophages in erythroblastic islands. Blood. 2014;123(25):3963–3971.
24. Dransfield, I., Zagórska, A., Lew, E., Michail, K. and Lemke, G. (2015). Mer receptor tyrosine kinase mediates both tethering and phagocytosis of apoptotic cells. *Cell Death and Disease*, 6(2), p.e1646.
25. Healy, L. M., Perron, G., Won, S.-Y., Michell-Robinson, M. A., Rezk, A., Ludwin, S. K., Moore, C. S., Hall, J. A., Bar-Or, A., and Antel, J. P. (2016) MerTK Is a Functional Regulator of Myelin Phagocytosis by Human Myeloid Cells. *The Journal of Immunology*. 196, 3375–3384.
26. Shooner, C., Caron, P-L, Fréchette-Frigon, G., Leblanc, V., Déry, M-C, Asselin, E. (2005) TGF-beta expression during rat pregnancy and activity on decidual cell survival. *Reproductive biology and endocrinology :* 20.

27. Pijnenborg, R., McLaughlin, P. J., Vercruysse, L., Hanssens, M., Johnson, P. M., Keith, J. C., & Van Assche, F. A. (1998). Immunolocalization of tumour necrosis factor-α (TNF-α) in the placental bed of normotensive and hypertensive human pregnancies. *Placenta*, *19*(4), 231–239.
28. Whitley, G. S. J., Dash, P. R., Ayling, L. J., Prefumo, F., Thilaganathan, B., & Cartwright, J. E. (2007). Increased apoptosis in first trimester extravillous trophoblasts from pregnancies at higher risk of developing preeclampsia. *American Journal of Pathology*, *170*(6), 1903–1909.
29. Robson, A., Harris, L. K., Innes, B. A., Lash, G. E., Aljunaidy, M. M., Aplin, J. D., … Bulmer, J. N. (2012). Uterine natural killer cells initiate spiral artery remodeling in human pregnancy. *FASEB Journal*, *26*(12), 4876–4885.
30. Whitley, G. S. J., & Cartwright, J. E. (2009). Trophoblast-mediated spiral artery remodelling: A role for apoptosis. *Journal of Anatomy*, *215*(1), 21–26. http://doi.org/10.1111/j.1469-7580.2008.01039.x
31. Nishi, C., Toda, S., Segawa, K., & Nagata, S. (2014). Tim4- and MerTK-Mediated Engulfment of Apoptotic Cells by Mouse Resident Peritoneal Macrophages. *Molecular and Cellular Biology*, *34*(8), 1512–1520. http://doi.org/10.1128/MCB.01394-13
32. Kamińska, A., Enguita, F. J., & Stępień, E. (2017). Lactadherin: An unappreciated haemostasis regulator and potential therapeutic agent. *Vascular Pharmacology*, *101*(December), 21–28. http://doi.org/10.1016/j.vph.2017.11.006
33. Fuller, A. D., & Van Eldik, L. J. (2008). MFG-E8 regulates microglial phagocytosis of apoptotic neurons. *Journal of Neuroimmune Pharmacology*, *3*(4), 246–256. http://doi.org/10.1007/s11481-008-9118-2
34. Valdés, G. (2017). Preeclampsia and cardiovascular disease: Interconnected paths that enable detection of the subclinical stages of obstetric and cardiovascular diseases. *Integrated Blood Pressure Control*, *10*, 17–23.
35. Staff, A. C., Dechend, R., & Pijnenborg, R. (2010). Learning from the placenta: Acute atherosis and vascular remodeling in preeclampsia-novel aspects for atherosclerosis and future cardiovascular health. *Hypertension*, *56*(6), 1026–1034.
36. Moore, K. J., Sheedy, F. J., and Fisher, E. A. (2013) Macrophages in atherosclerosis: A dynamic balance. *Nat. Rev. Immunol.* **13**, 709–721
37. Zhu, J., Wang, K., Li, T., Chen, J., Xie, D., Chang, X., Yao, J., Wu, J., Zhou, Q., Jia, Y., and Duan, T. (2017) Hypoxia-induced TET1 facilitates trophoblast cell migration and invasion through HIF1α signaling pathway. *Sci. Rep.* **7**, 1–11
38. Sherer, M. L., Khanal, P., and Schwarz, J. M. Rat model of Prenatal Zika virus infection. *Brain Behav. Immun.* **66**, e11
39. Crittenden, M. R., Baird, J., Friedman, D., Savage, T., Uhde, L., Alice, A., Cottam, B., Young, K., Newell, P., Nguyen, C., Bambina, S., Kramer, G.,

Akporiaye, E., Malecka, A., Jackson, A., and Gough, M. J. (2014) Mertk on tumor macrophages is a therapeutic target to prevent tumor recurrence following radiation therapy. *Oncotarget*. 10.18632/oncotarget.11823

40. Hartley, G., Regan, D., Guth, A., and Dow, S. (2017) Regulation of PD-L1 expression on murine tumor-associated monocytes and macrophages by locally produced TNF-α. *Cancer Immunol. Immunother.* **66**, 523–535
41. Pang, Y., Gara, S. K., Achyut, B. R., Li, Z., Yan, H. H., Day, C.-P., Weiss, J. M., Trinchieri, G., Morris, J. C., and Yang, L. (2013) TGFβ Signaling in Myeloid Cells Is Required for Tumor Metastasis. *Cancer Discovery*. **3**, 936–951Soki, F. N., Koh, A. J., Jones, J. D., Kim, Y. W., Dai, J., Keller, E. T., Pienta, K. J., Atabai, K., Roca, H., and McCauley, L. K. (2014) Polarization of prostate cancer-associated macrophages is induced by milk fat globule-EGF factor 8 (MFG-E8)-mediated efferocytosis. *J. Biol. Chem.* **289**, 24560–24572
42. Flecken, T., and Sarobe, P. (2015) Tim-3 expression in Tumour-associated macrophages: A new player in HCC progression. *Gut*. **64**, 1502–1503
43. Gabrilovich, D. I., and Nagaraj, S. (2009) Myeloid-derived-suppressor cells as regulators of the immune system. *Nat. Rev. Immunol.* **9**, 162–174